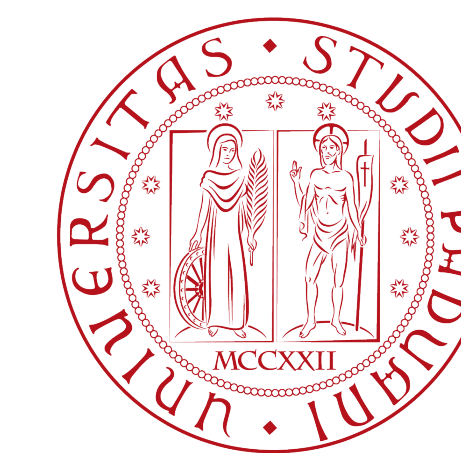


The cosmic merger rate density of compact binaries

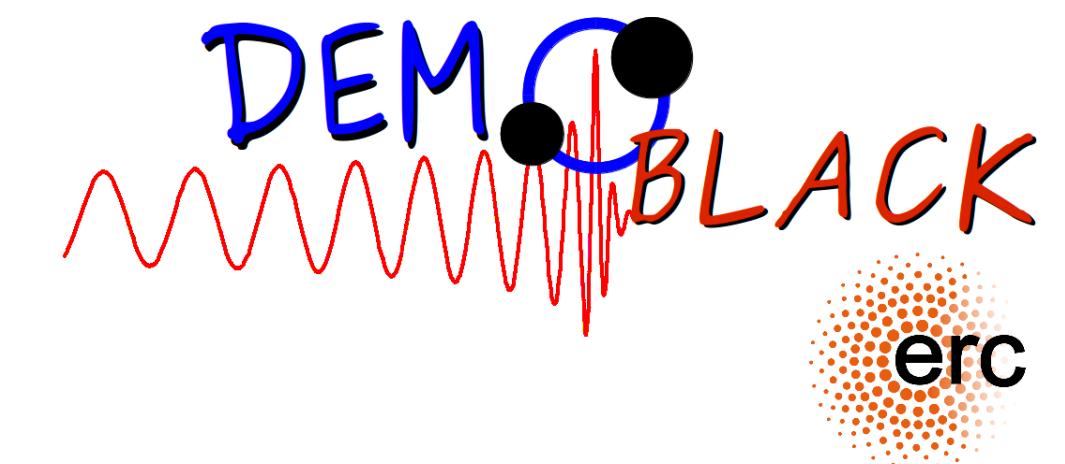
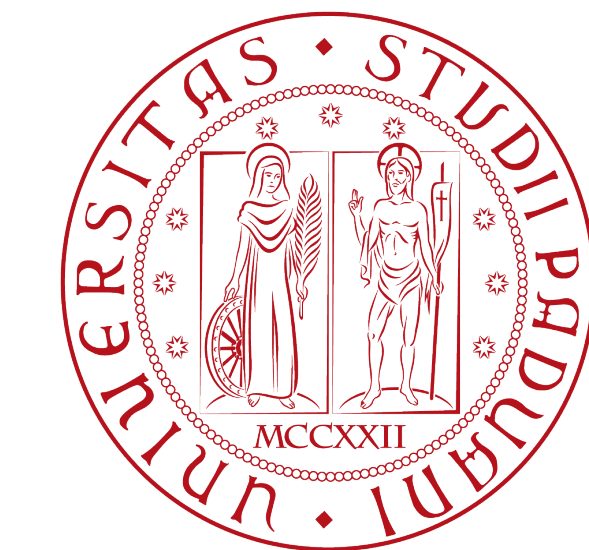
Filippo Santoliquido

IAP/APC high-energy Journal Club - June 24, 2021



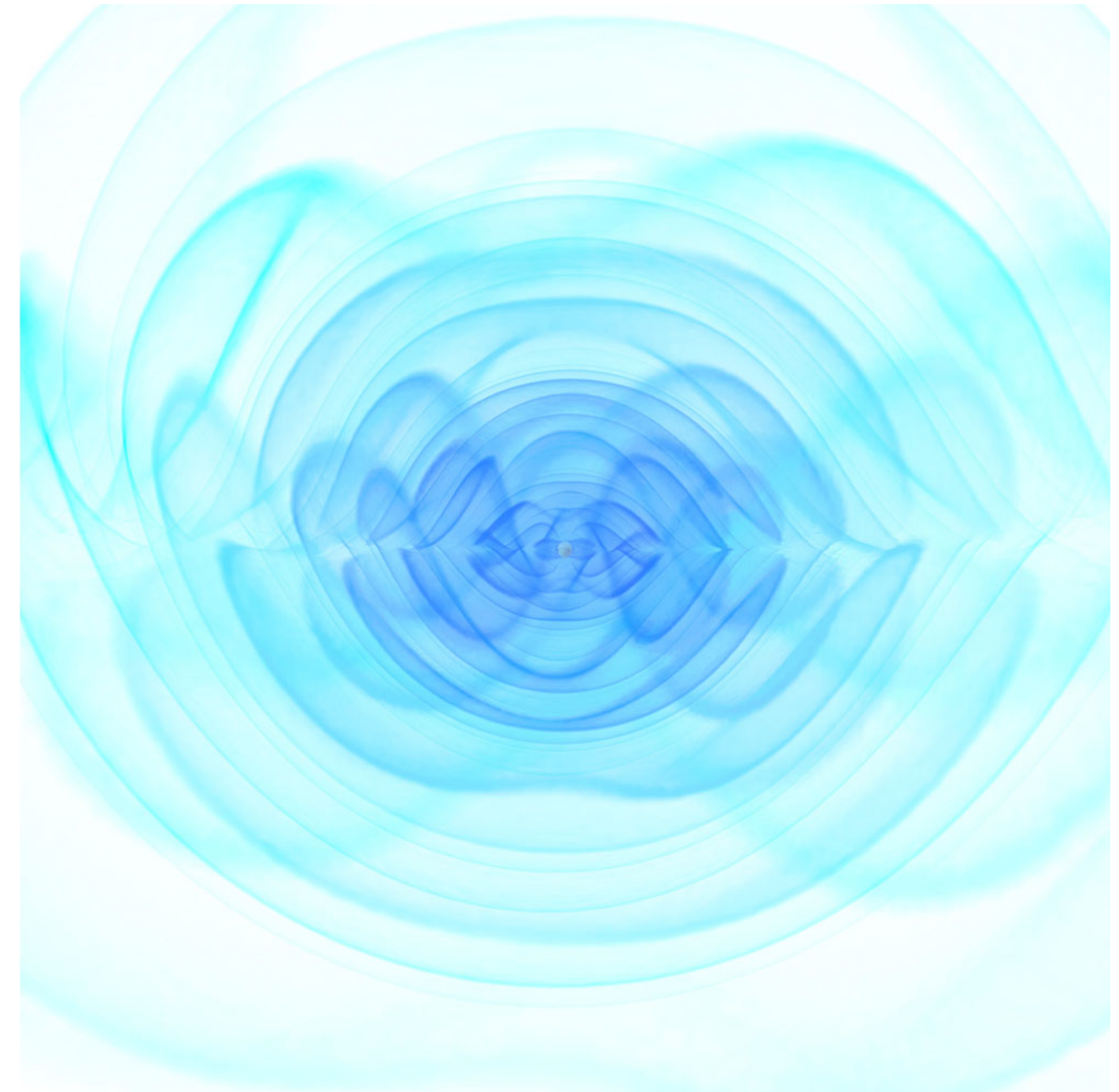
Let introduce myself

- I graduated in Astronomy at the end of 2019
- Now, I am a PhD student of the University of Padova
- I completed roughly 50% of my PhD
- My supervisor is prof. Michela Mapelli and I work in her research group: **DEMOBLACK**
www.demoblack.com
- If you'd like to contact me, please write me at
filippo.santoliquido@phd.unipd.it

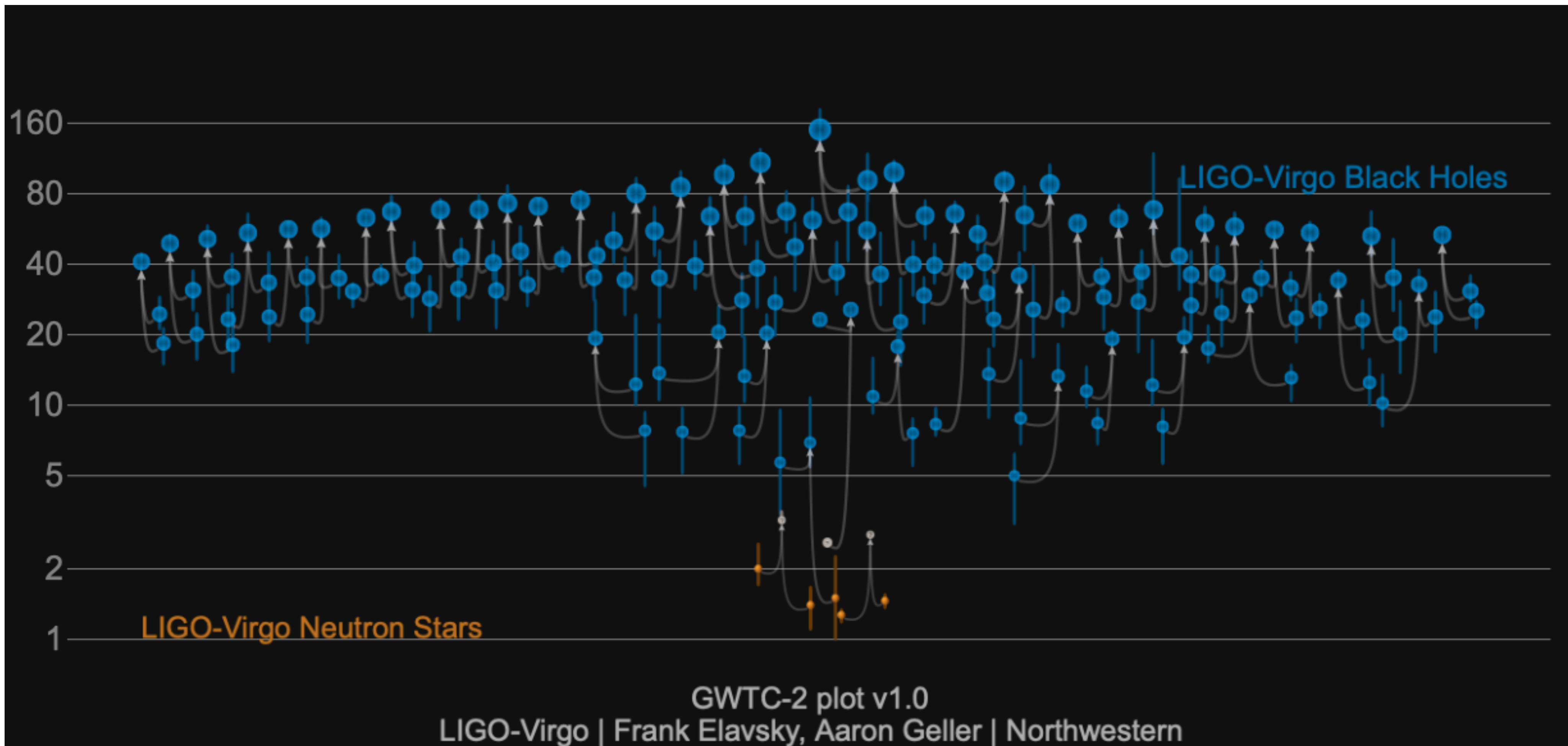


Outline

1. Gravitational wave (GW) **detections** and inferred **population properties** of merging compact objects
2. **Astrophysical models** of compact binaries. Focus on formation channels.
3. A semi-analytic model to evaluate the merger rate density (***my own work***)
4. **Comparison** of population models with observations

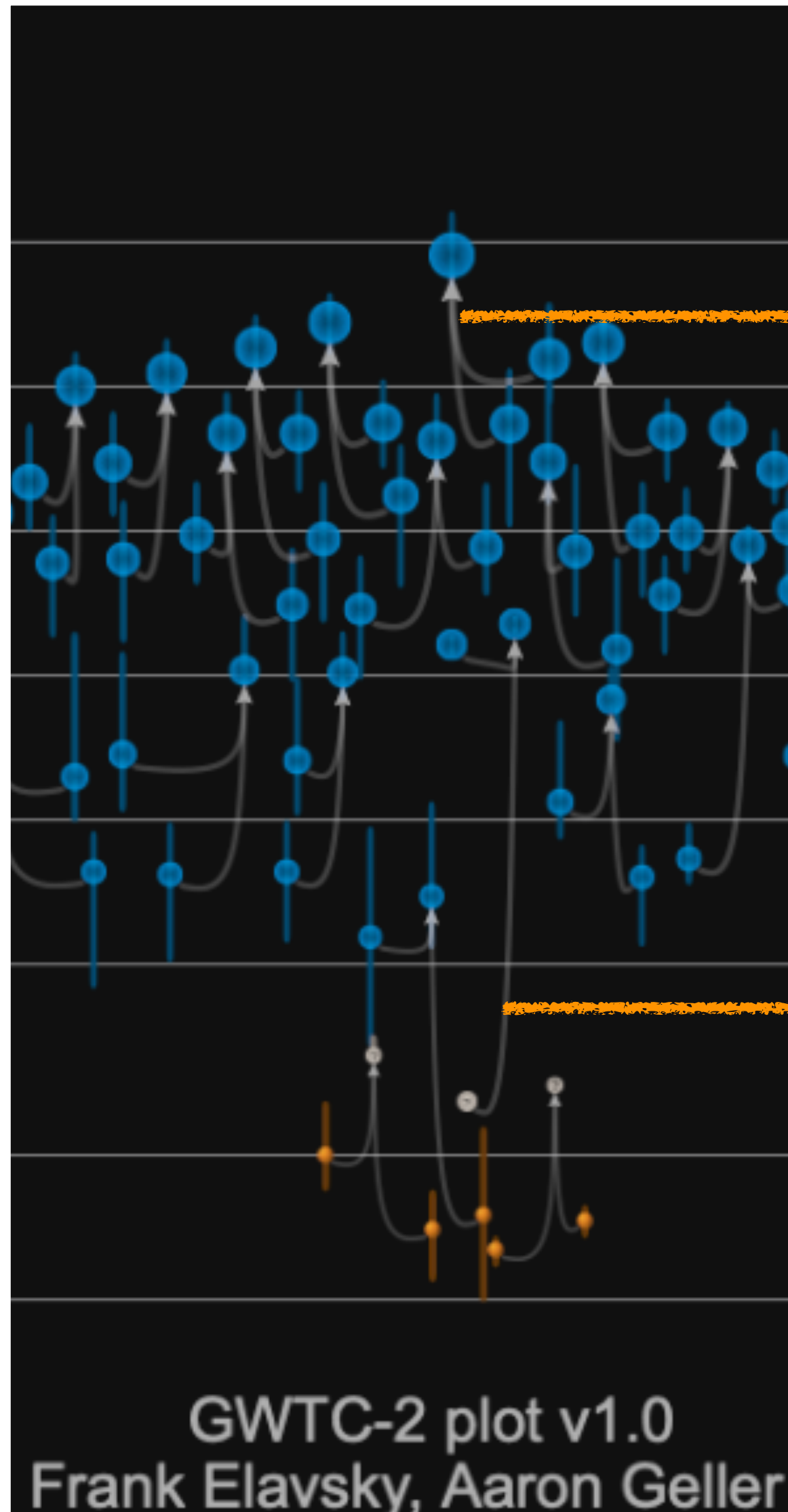


The population of detected binaries



Abbott et al. 2020, GWTC-2, 2020, <https://arxiv.org/abs/2010.14527>

Two peculiar mergers

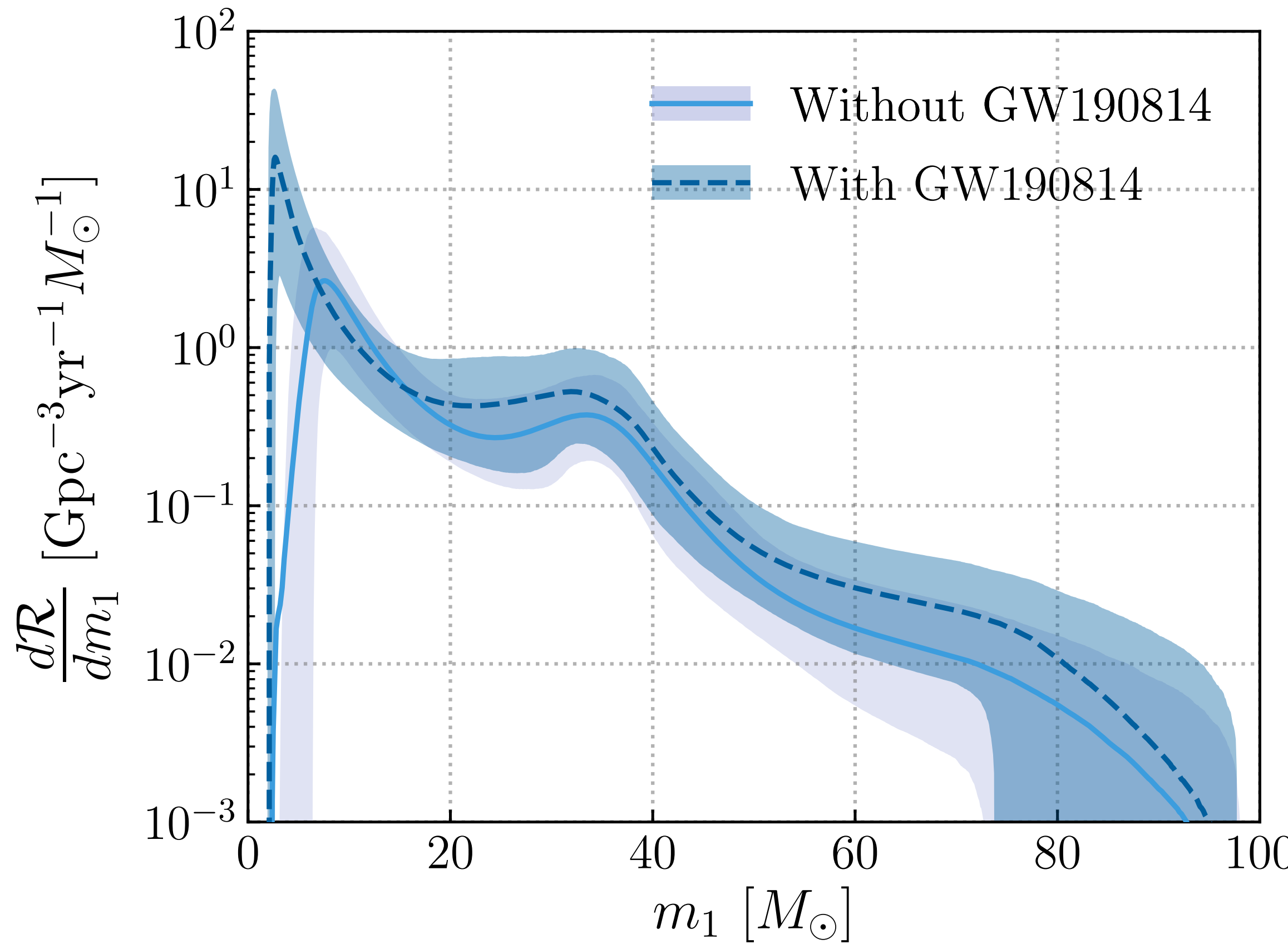


GW190521 - most massive GW event to date:
total mass $\sim 150 M_{\odot}$

And primary mass in the pair instability mass gap
(*Abbott et al. 2020, discovery, <https://arxiv.org/abs/2009.01075>*
Abbott et al. 2020, implications, <https://arxiv.org/abs/2009.01190>)

GW190814 - secondary mass lies in the first
mass gap, object with the greatest mass ratio -
(*Abbott et al. 2020, <https://arxiv.org/abs/2006.12611>*)

Merger rate density inferred from GW detections



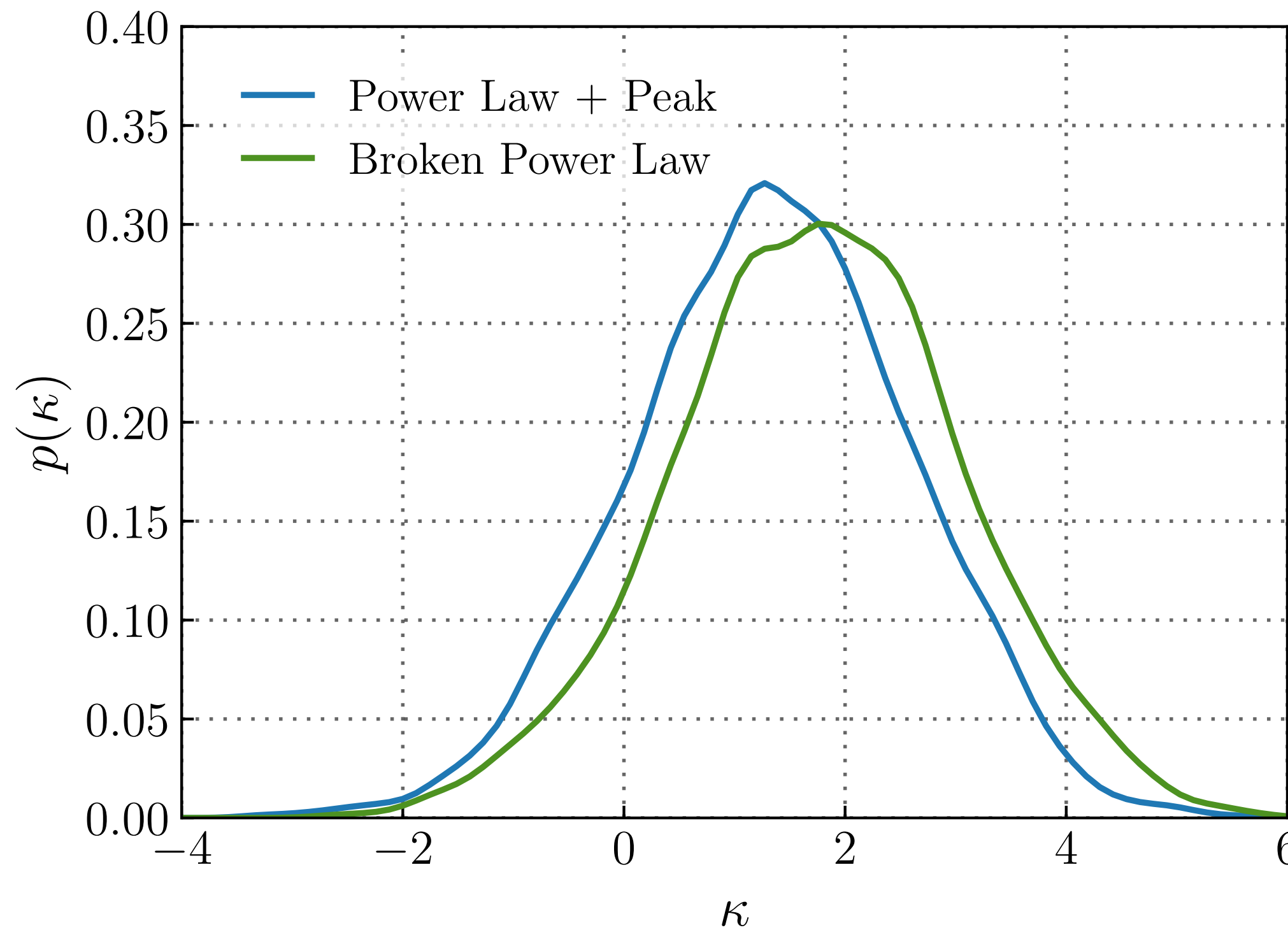
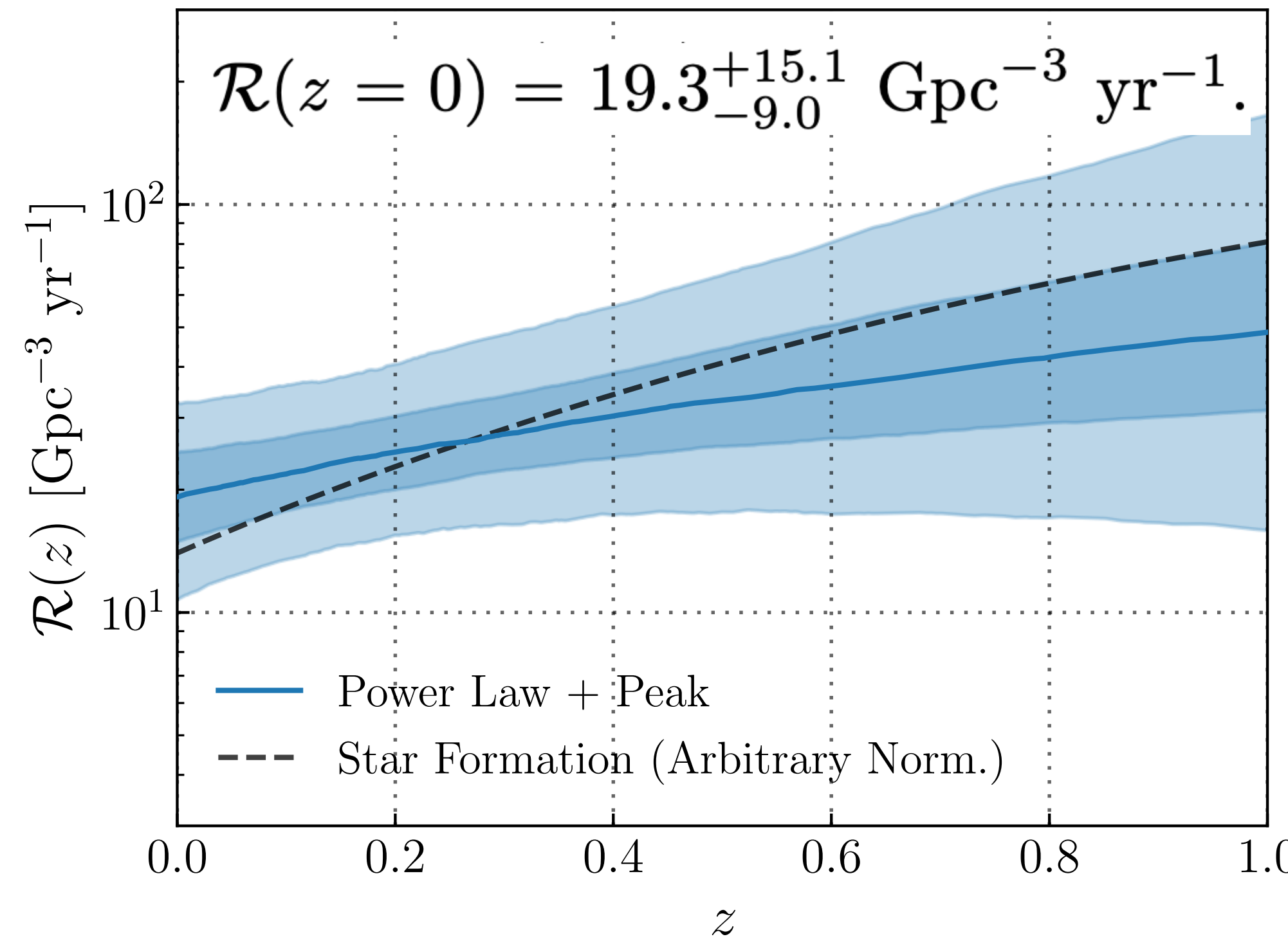
Power Law + Peak mass distribution model

- $\mathcal{R}_{\text{BBH}} = 23.9^{+14.9}_{-8.6} \text{ Gpc}^{-3} \text{ yr}^{-1}$
(without GW190814)
- $\mathcal{R}_{\text{BBH}} = 58^{+54}_{-29} \text{ Gpc}^{-3} \text{ yr}^{-1}$
(with GW190814)

Abbott et al. 2021b, <https://arxiv.org/abs/2010.14533>

Merger rate density as a function of redshift

- Let's assume the merger rate density varies as $\mathcal{R} \propto (1 + z)^k$, i.e. it has the same trend as the star formation rate density
- At 85% credibility the merger rate is increasing with redshift ([Abbott et al. 2021b, <https://arxiv.org/abs/2010.14533>](https://arxiv.org/abs/2010.14533))



How gravitational wave sources form?

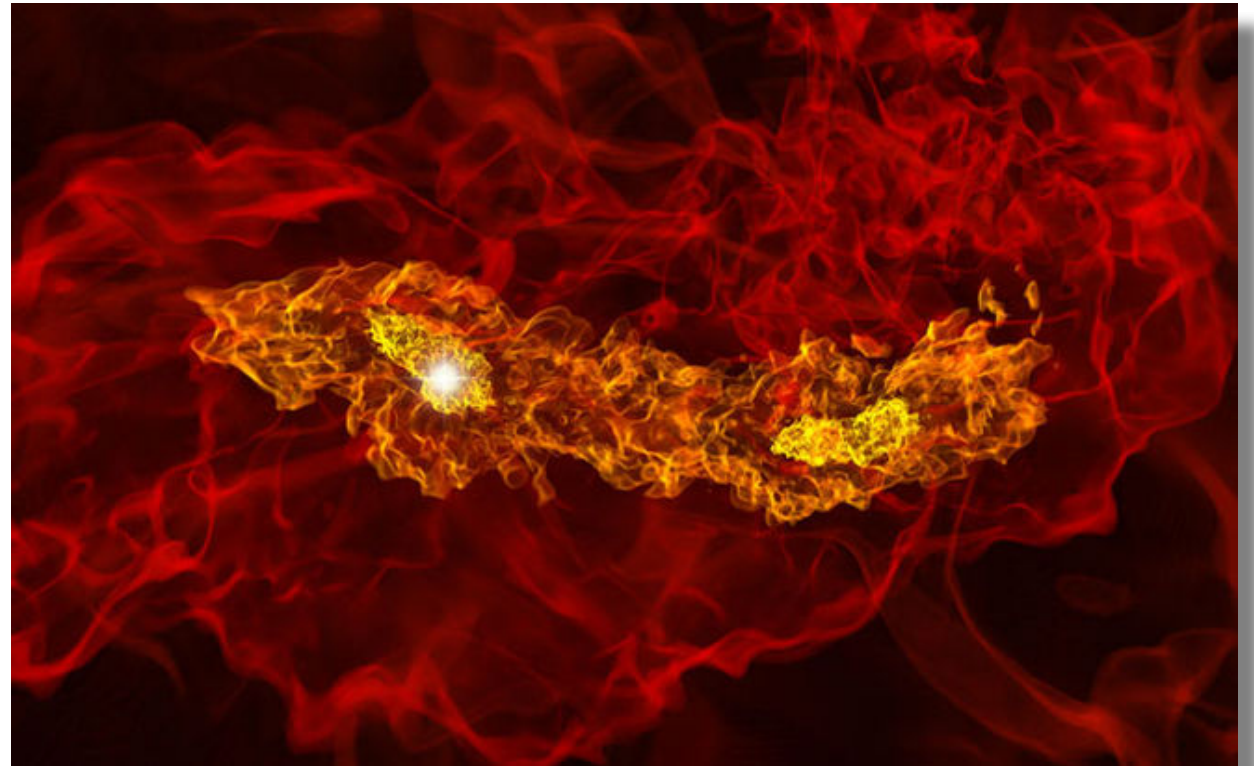
Single stellar evolution:

Black holes and neutron stars are the final step of massive stars evolution

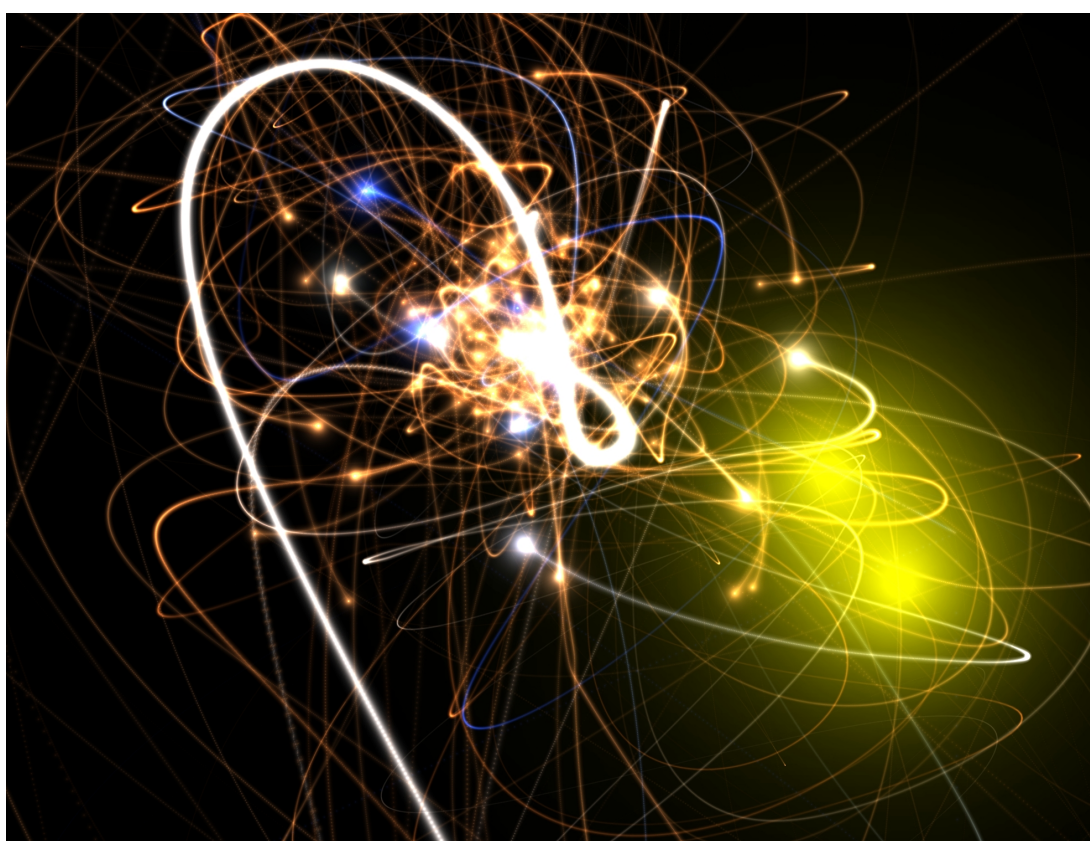


Isolated formation channel:

two stars evolve into two compact objects



Credits: A. Geller



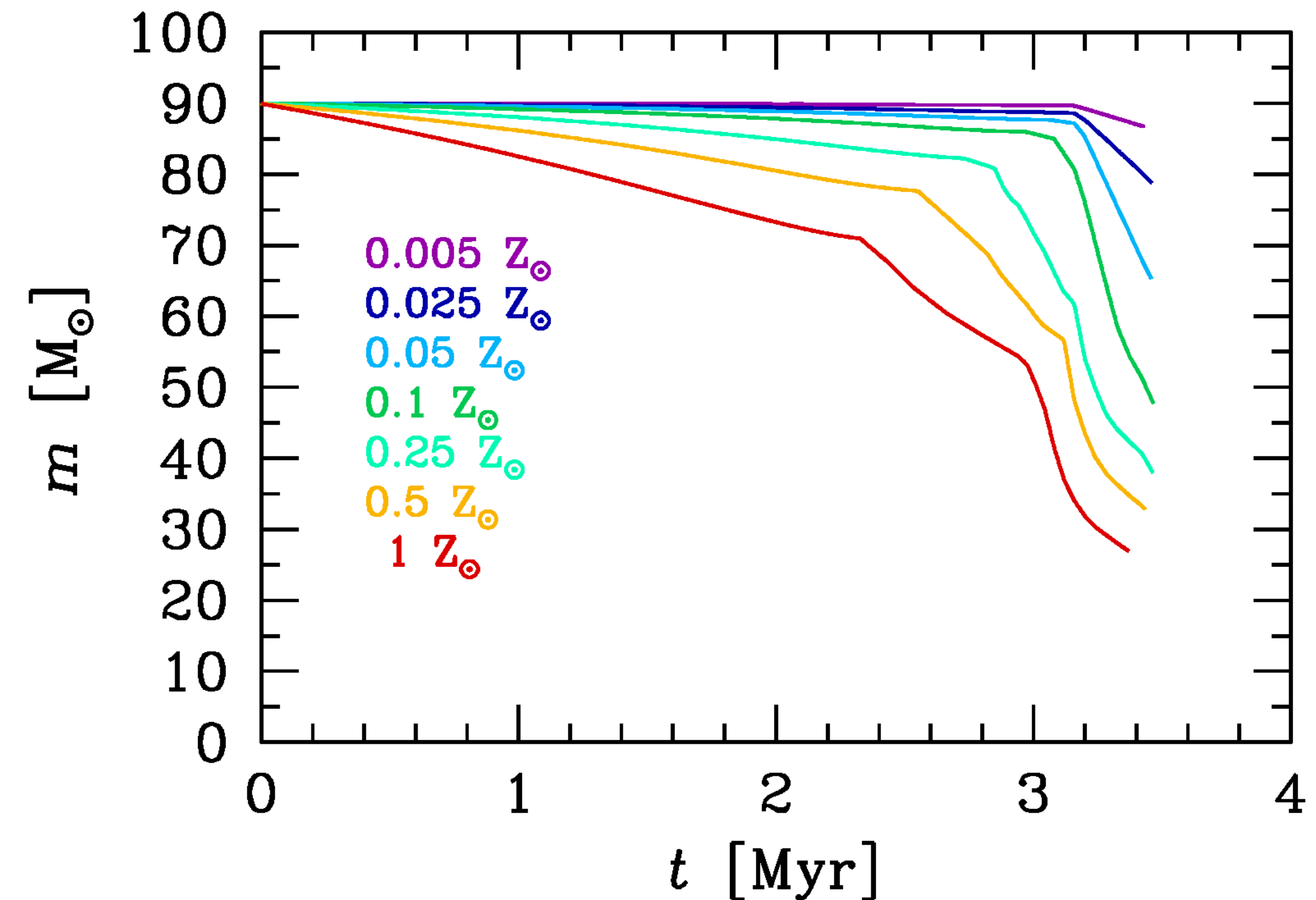
Dynamical formation channel:

Binary compact objects
form and/or evolve
by dynamical processes
in star clusters

Credits: Turk, Abel, O'Shea 2009

Single stellar evolution: stellar winds

- Massive stars lose mass by **stellar winds** which depend on **metallicity** and **Eddington ratio** (e.g. [Vink et al. 2001](#); [Graefener & Hamann 2008](#); [Vink et al. 2011](#))
- $\dot{M} \propto Z^\alpha$, where
 $\alpha = 0.85$ if $\Gamma < 2/3$, $\alpha = 2.45 - 2.4\Gamma$ if $\Gamma > 2/3$ where $\Gamma = \frac{L_*}{L_{\text{Edd}}}$
[Chen, Bressan et al. \(2015\)](#)
- Since **metal-poor stars** have larger pre-supernova masses they are also more likely to directly collapse, producing **more massive black holes** ([Heger et al. 2003](#); [MM et al. 2009, 2010, 2013](#); [Belczynski et al. 2010](#); [Fryer et al. 2012](#))



[Mapelli, 2018](#)

Single stellar evolution: pair instability mass gap

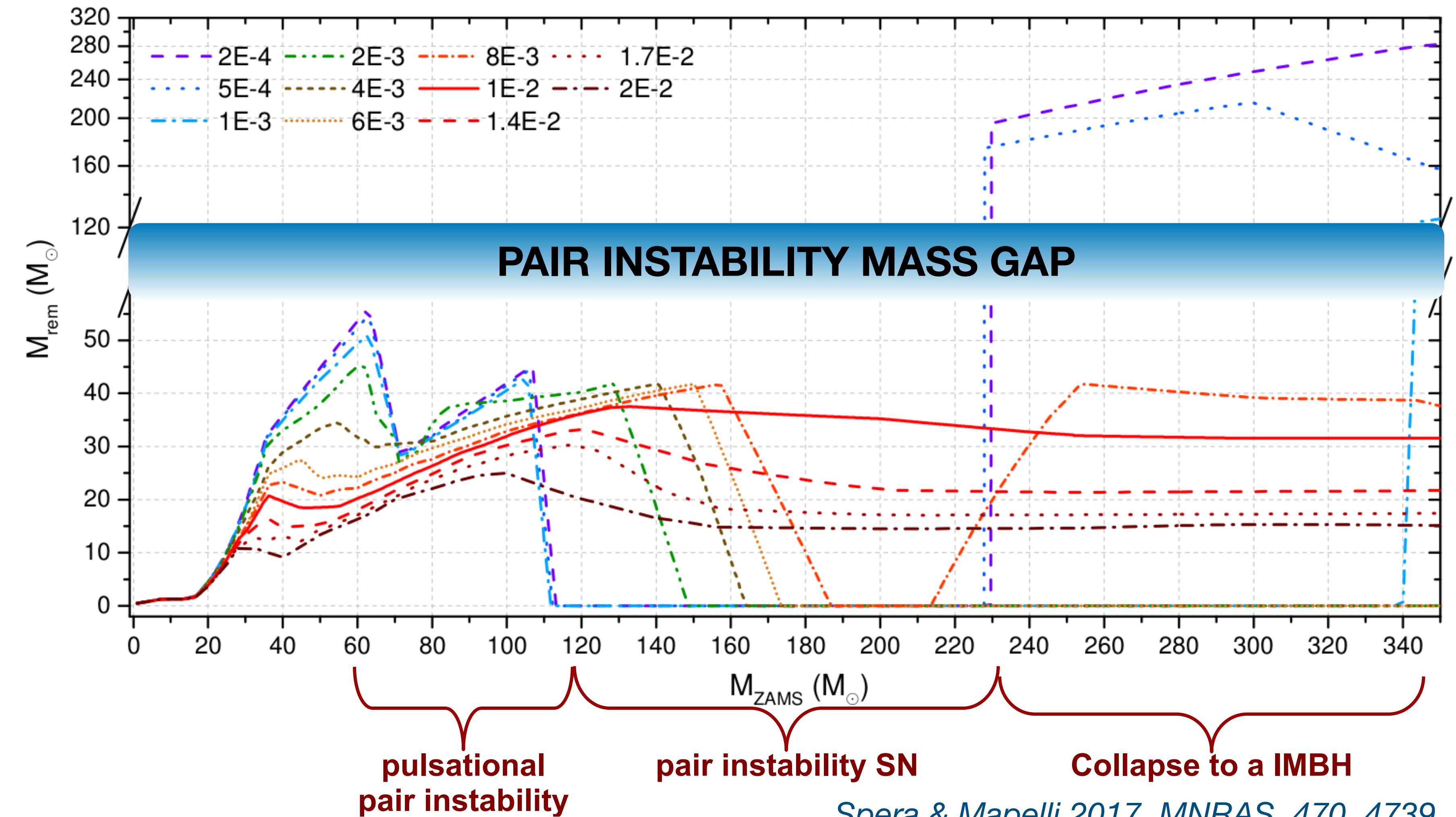
Main phenomenon: **pair production**

$(\gamma \rightarrow e^- + e^+)$ reduces the internal **radiation pressure**

pulsational pair instability
 $(32 < m_{He}/M_\odot < 64)$

pair instability SN
 $(64 < m_{He}/M_\odot < 135)$

Costa et al. 2021,
MNRAS, 501, 4514



Isolated formation channel: main physical processes

- In the **isolated formation channel**, we focus on the evolution of a two-star system
- **mass transfer** during Roche lobe overflow, whose efficiency is determined by the mass accretion efficiency parameter (f_{MT})
- **SN** which are followed by **natal kicks**. These are especially relevant for BNSs.
- **Common envelope** phase, described by the $\alpha\lambda$ -formalism
- We explored the impact of several different parameters

Explored parameters

Initial Mass Function



Mass transfer
(f_{MT})



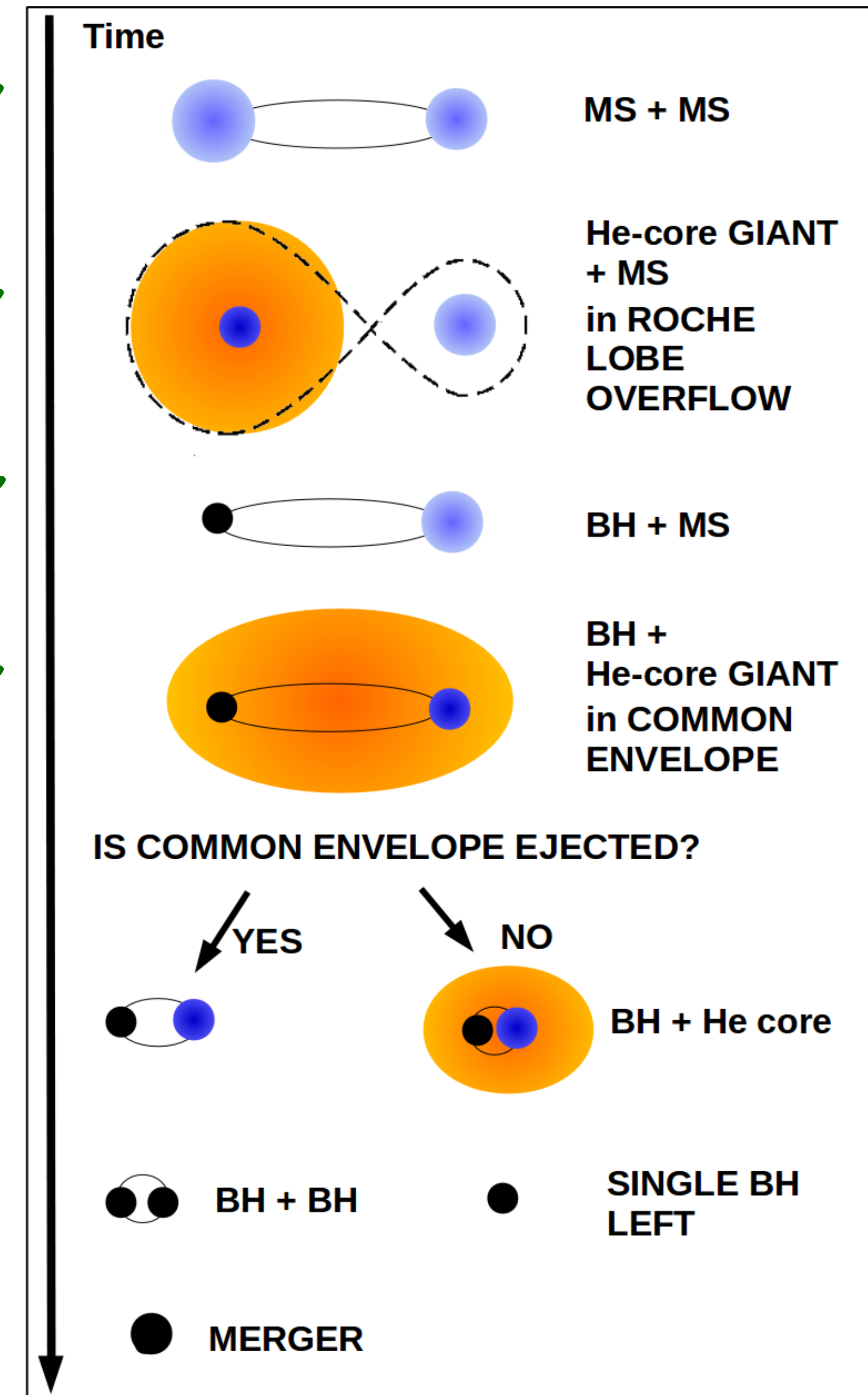
SN model and
Natal kicks



Common
Envelope

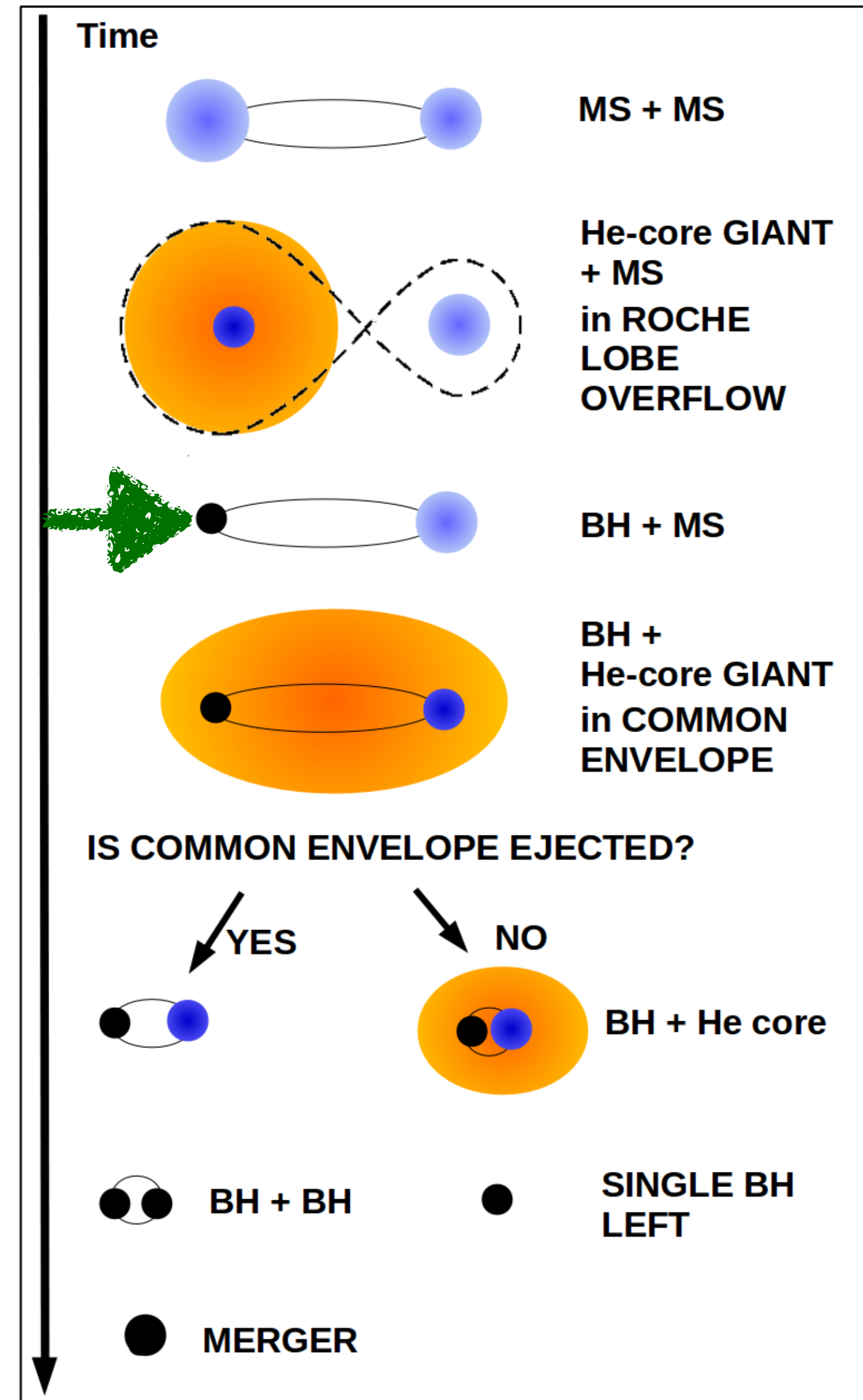


Example



Mapelli, 2018

Example



[Mapelli, 2018](#)

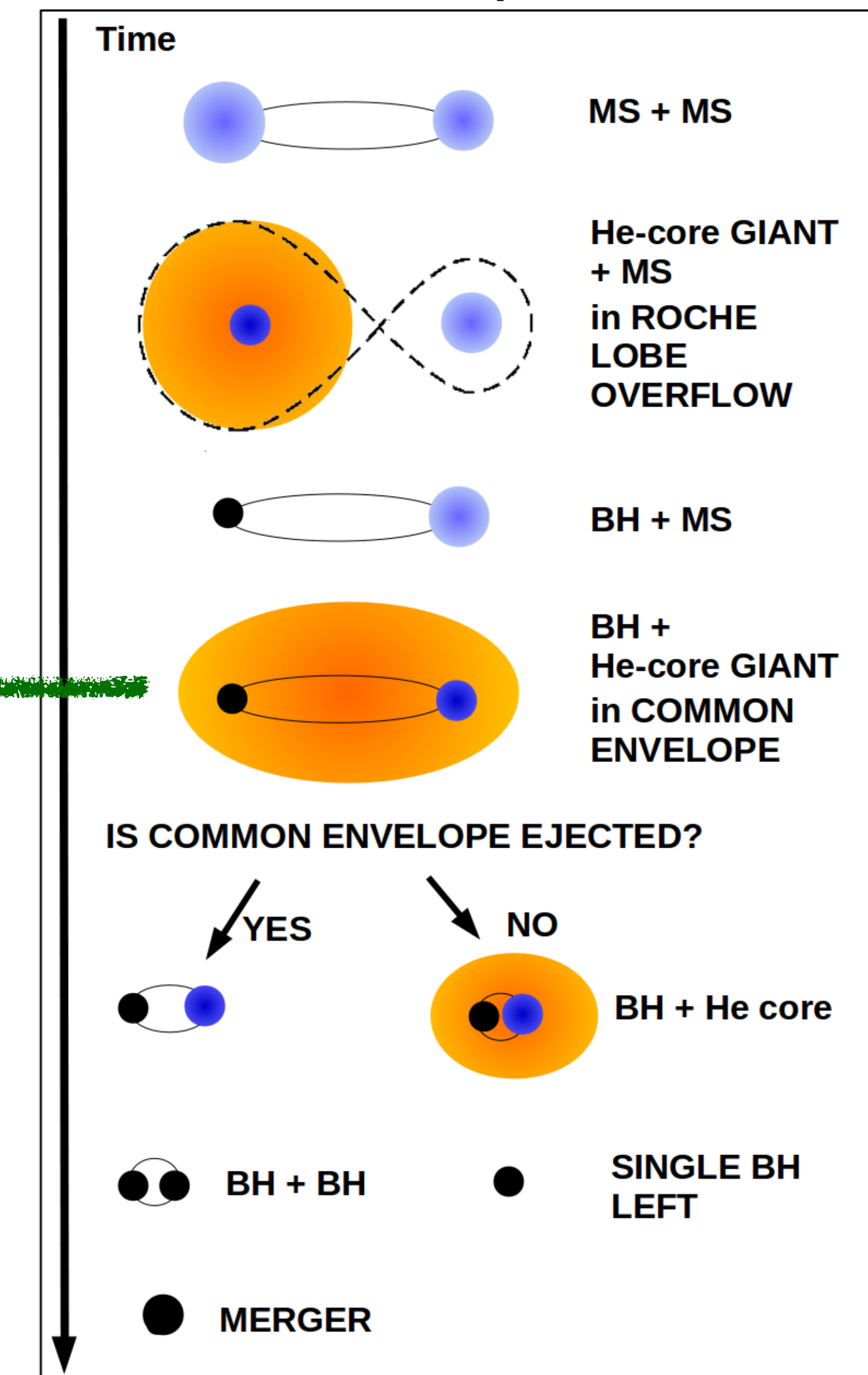
Isolated formation channel: natal kicks

- In [Santoliquido et al. 2021](#) we compared four natal kicks models:

1. Natal kicks drawn from single maxwellian distributions with $\sigma = 265 \text{ km s}^{-1}$ (f_{H05} from [Hobbs et al. 2005](#)), 150 km s^{-1} , 50 km s^{-1}
2. The [Fryer et al. 2012](#) model $v_{kick} = (1 - f_{fb})f_{H05}$. The fallback is the fraction of stellar mass that falls back to the remnant.
3. The [Vigna-Gómez et al. 2018](#) model: two different maxwellian distributions: $\sigma_{CCSN} = 265 \text{ km s}^{-1}$ for CCSN and $\sigma_{ECSN} = 30 \text{ km s}^{-1}$ for ECSN.
4. Our fiducial model is [Giacobbo et al. 2020](#):

$$v_{kick} = f_{H05} \frac{m_{ej}}{\langle m_{ej} \rangle} - \frac{\langle m_{NS} \rangle}{m_{rem}}$$

Example

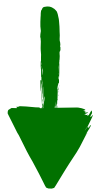


Mapelli, 2018

Isolated formation channel: common envelope

- Common envelope phase is described by the $\alpha\lambda$ -formalism
- The final radius of the binary after the CE phase (a_{fin}) is determined by the following equation
- $$\alpha \left(-\frac{Gm_1m_2}{2a_{ini}} + \frac{Gm_{1,core}m_2}{2a_{fin}} \right) = \frac{m_1m_{1,env}}{R_1\lambda}$$
- Where α parametrises the efficiency of transferring the energy from the binary internal energy to the CE bound energy. In [Santoliquido et al. 2021](#) we chose values from $\alpha = 0.5$ to $\alpha = 10$

Isolated binaries through population-synthesis



Very large statistical samples of merging compact binaries.

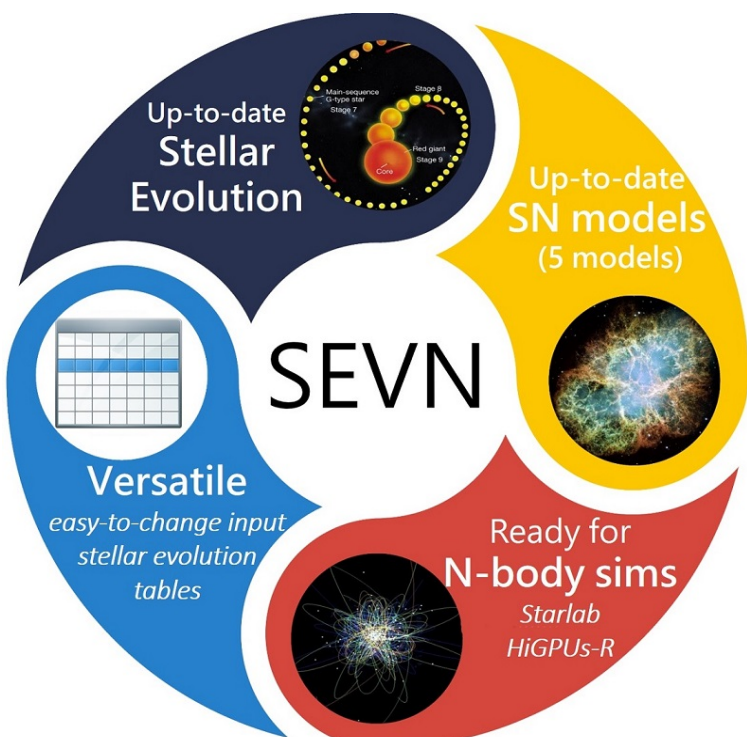


By using approximate models for stellar evolution



MOBSE

([Mapelli et al. 2017](#); [Mapelli & Giacobbo 2018](#); [Giacobbo et al. 2018](#); [Giacobbo & Mapelli 2018](#); [Giacobbo & Mapelli 2020](#))



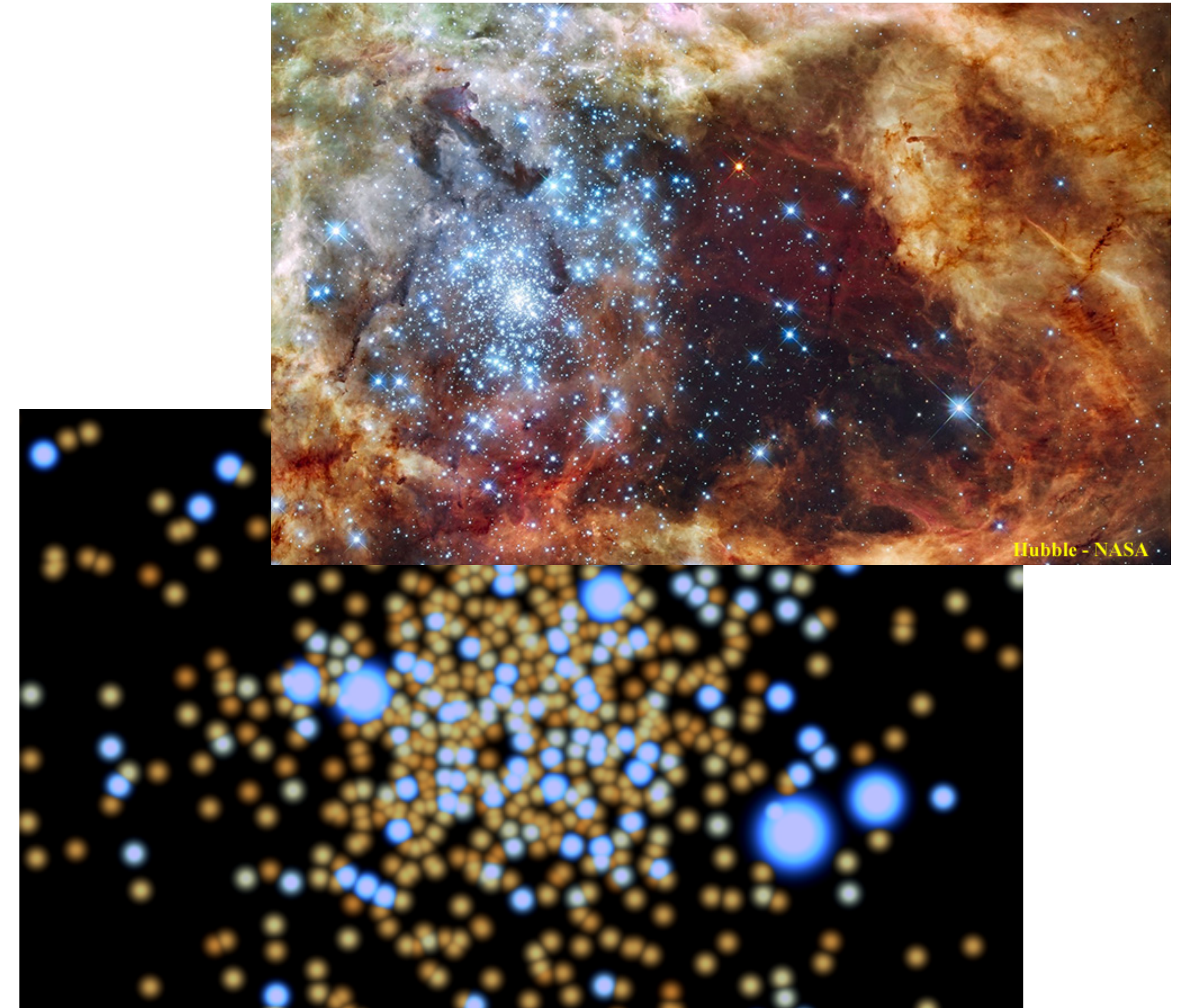
SEVN

([Spera, Mapelli & Bressan 2015](#); [Spera, Mapelli et al. 2019](#); [Mapelli et al. 2020](#))

You can download both codes at www.demoblack.com

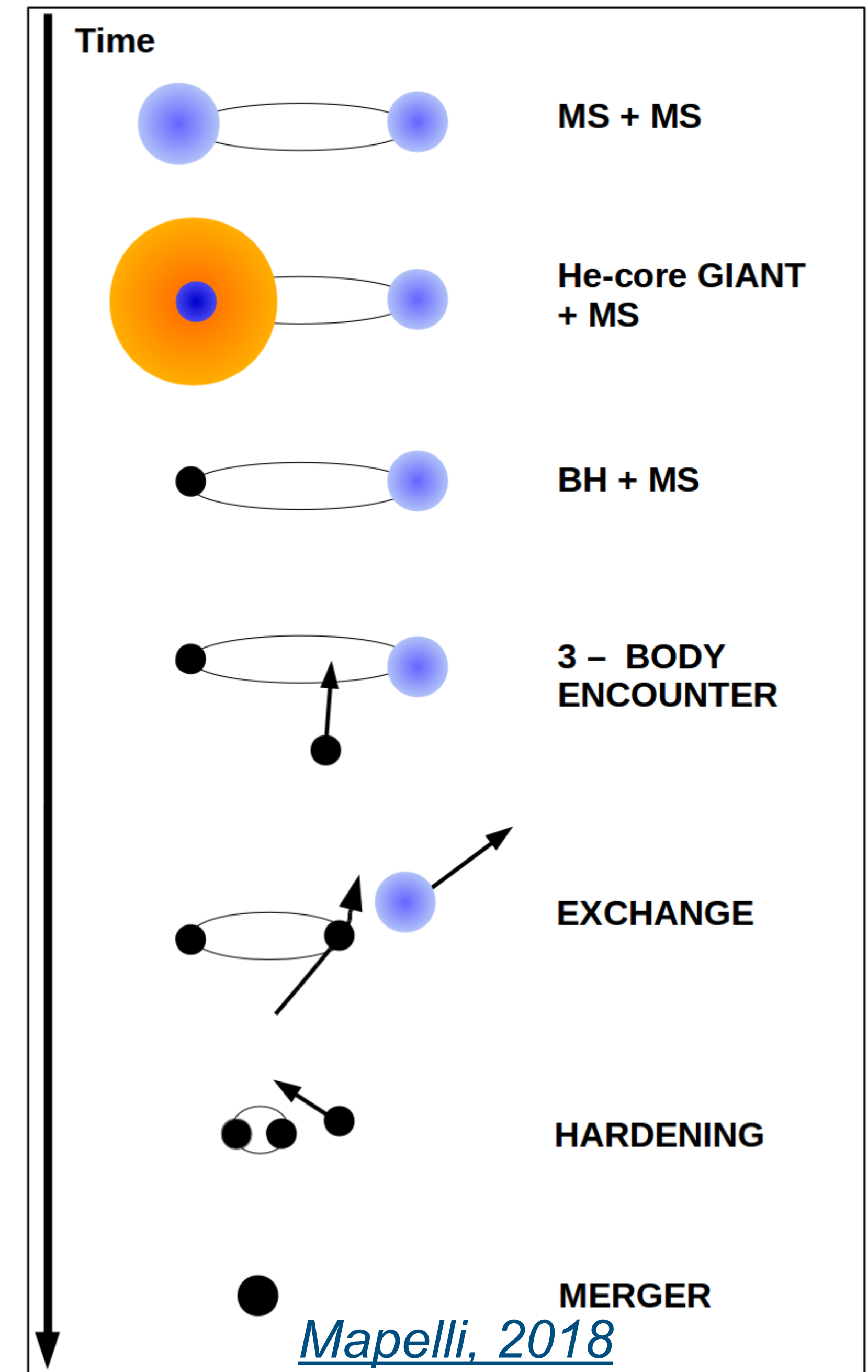
Dynamical binaries through N-body simulation

- Dynamics is important only if $n > 10^3$ stars/ pc^3 , i.e. only in dense star clusters
- We ran more than 10^5 simulations of **young star clusters** ($300 - 30'000 M_{\odot}$) ([Mapelli 2016](#); [Di Carlo et al. 2019](#) [Di Carlo et al. 2020a](#); [Di Carlo et al. 2020b](#) [Rastello et al. 2020](#), [Rastello et al. 2021](#))
- We combined **Nbody6++GPU** ([Wang et al. 2015, 2016](#)) with **MOBSE** ([Giacobbo and Mapelli, 2018](#)) to take into account binary evolution



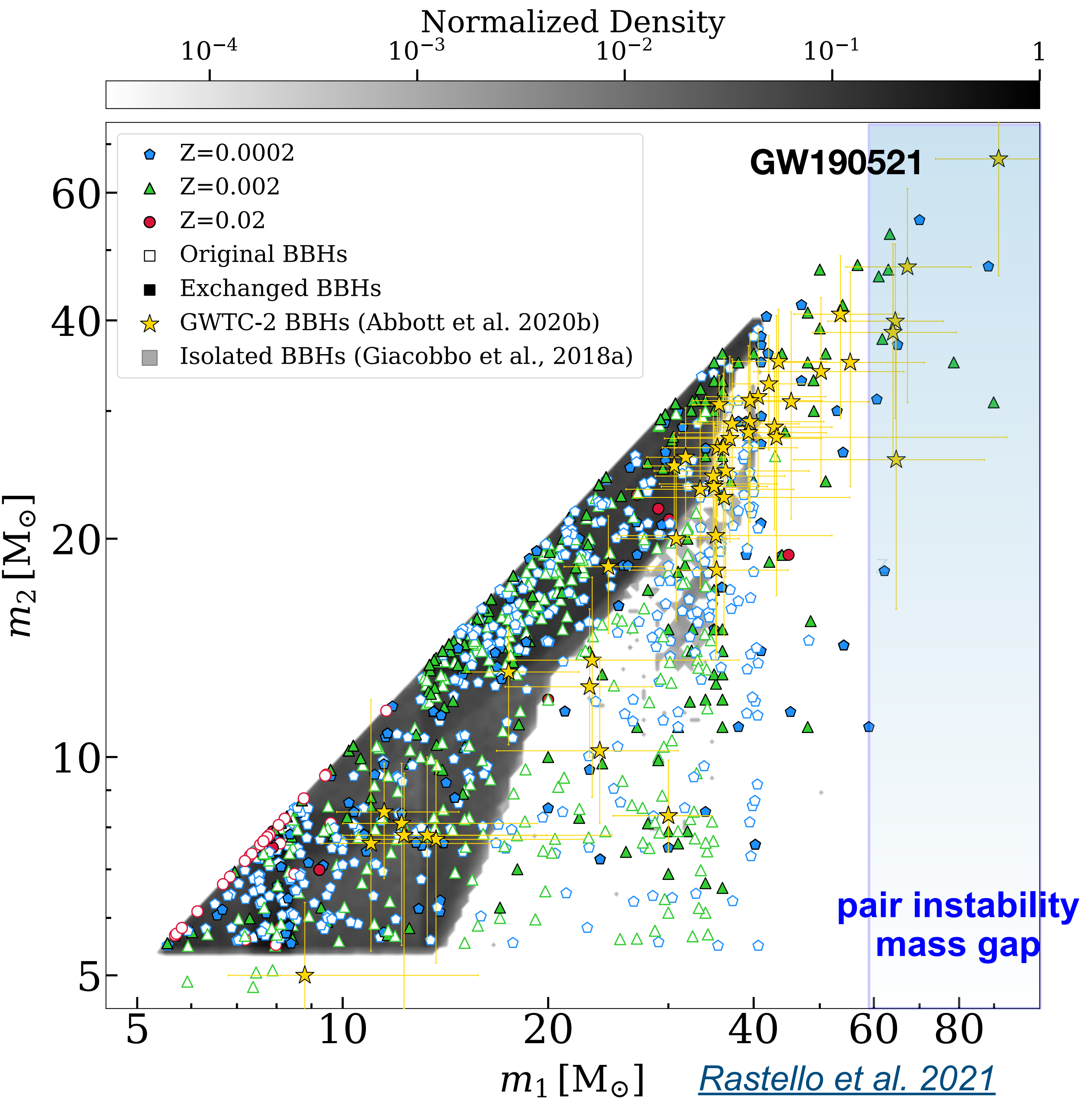
Dynamical formation channel: main physical process

- In a dynamical environment the binary can interact with a third body.
- The outcome of this interaction depends on several conditions ([*Dall'Amico et al. 2021*](#)):
 - ◆ **Exchanges** (we found that >50% BBHs in young star clusters form by exchange)
 - ◆ And **hardening** which help to further shrink the binary system



Comparison of these two populations: masses

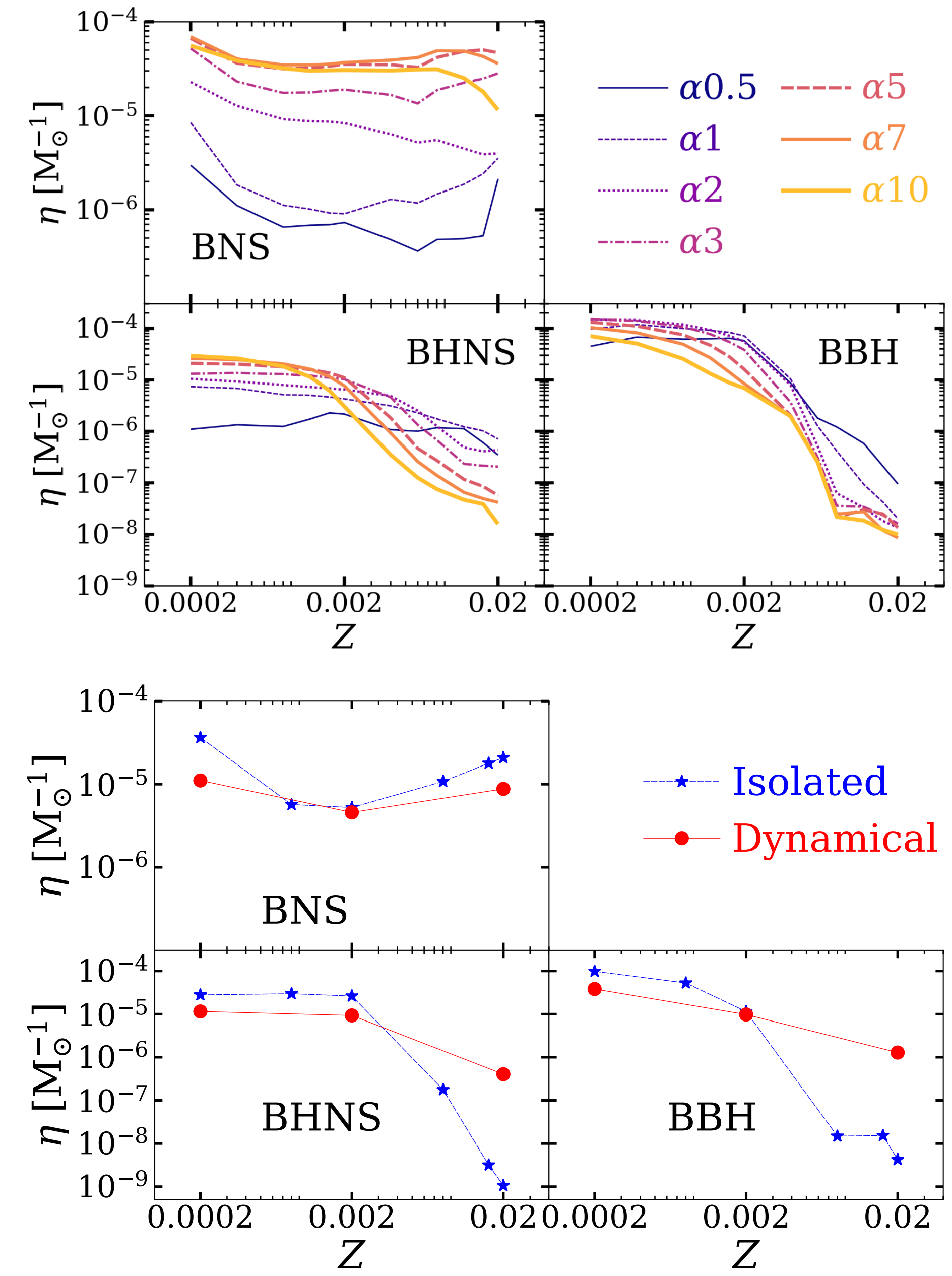
- **Isolated BBHs** can have total mass only up to $\sim 80 M_{\odot}$
- Instead: **dynamical BBHs** can have total mass $> 80 M_{\odot}$
- From the figure, we see that $\sim 1\%$ BBH have mass in the **pair instability mass gap**, corresponding to $\sim 5\%$ of **detectable events** ([Di Carlo et al. 2020a](#))
- very massive binaries can form only by **exchanges** and at sub-solar metallicity



The merger efficiency

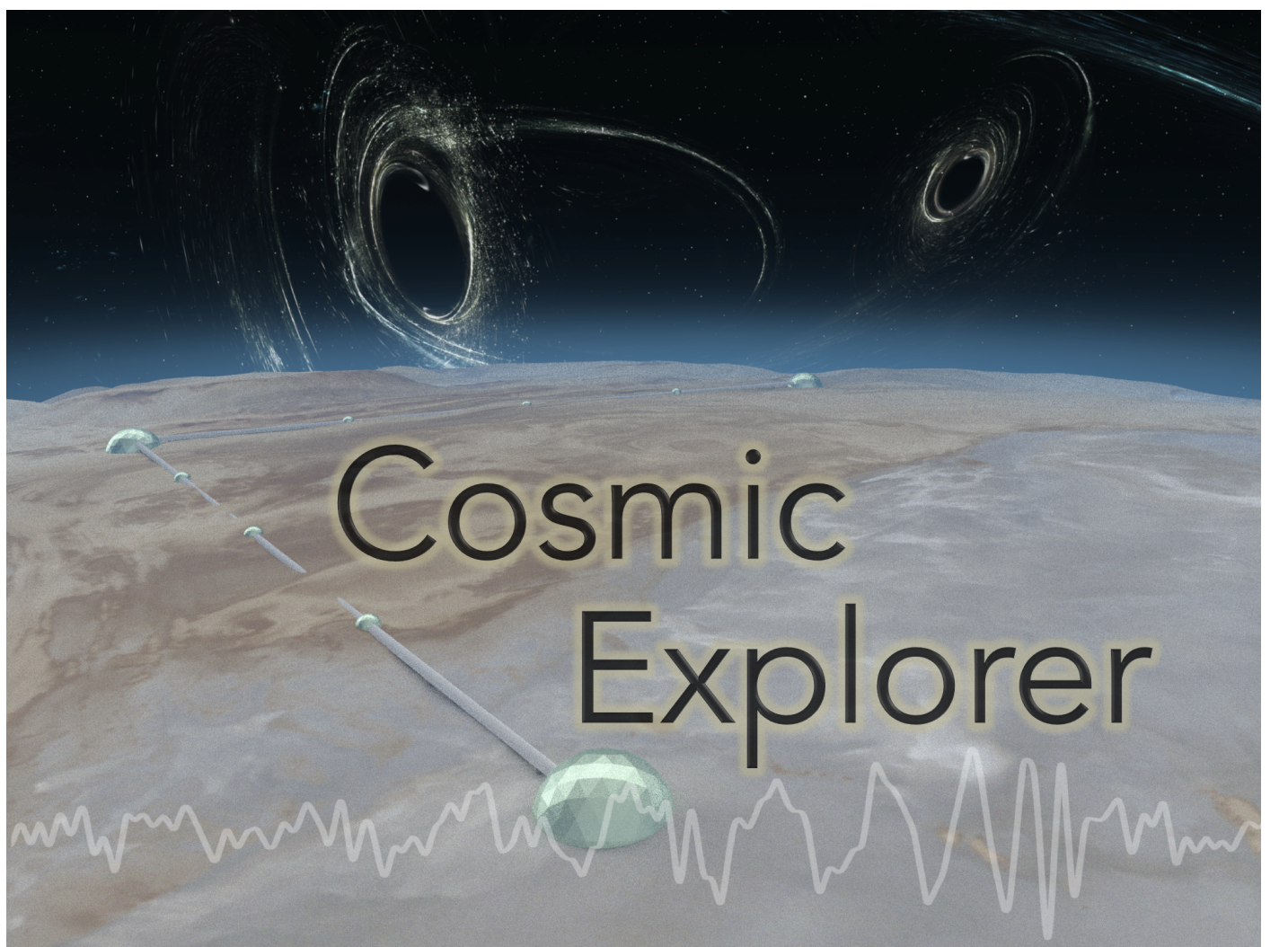
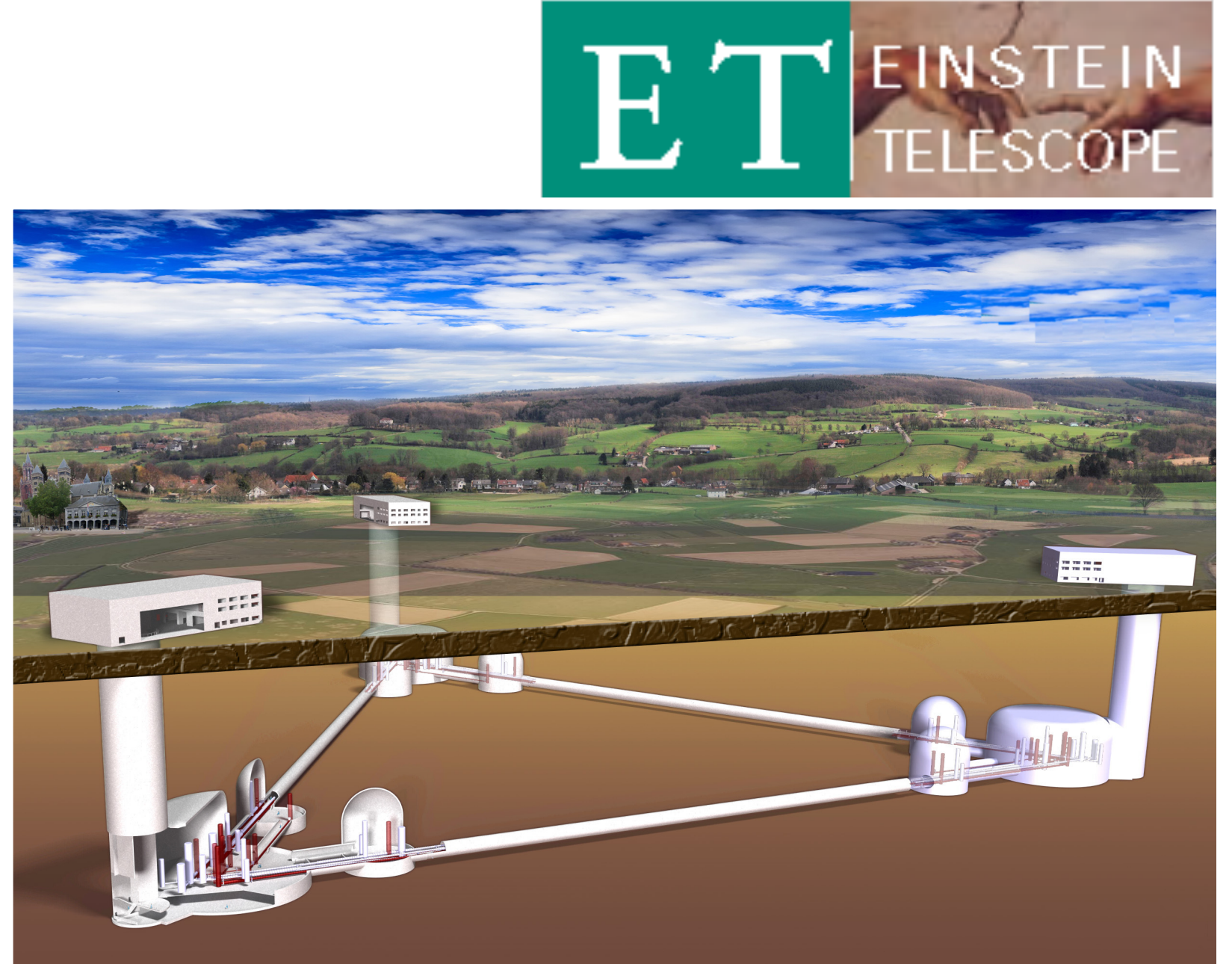
- $\eta = \frac{N_{TOT}}{M(Z)}$ where N_{TOT} are the number of binaries merging within an Hubble time
- This quantity gives us an idea of the impact of progenitor's metallicity on the merger rate density, in different scenarios
- The most interesting feature belongs to those binary which host a BH: the merger efficiency decreases by orders of magnitudes with increasing metallicity

Santoliquido et al. 2020, Santoliquido et al. 2021



The merger rate density across cosmic time

- From these populations of merging compact binaries we can evaluate the cosmic merger rate density
- We can compare it with the merger rate density inferred by the LIGO-Virgo collaboration in the local Universe.
- Future detections: 3G detectors will be able to detect mergers at $z > 10$ for BBHs and $z < 2$ for BNSs ([Punturo et al. 2010](#), [Reitze et al. 2019](#), [Kalogera et al. 2019](#), [Maggiore et al. 2020](#))
- Europe is planning to build the **Einstein Telescope**, while the US are planning the **Cosmic Explorer**

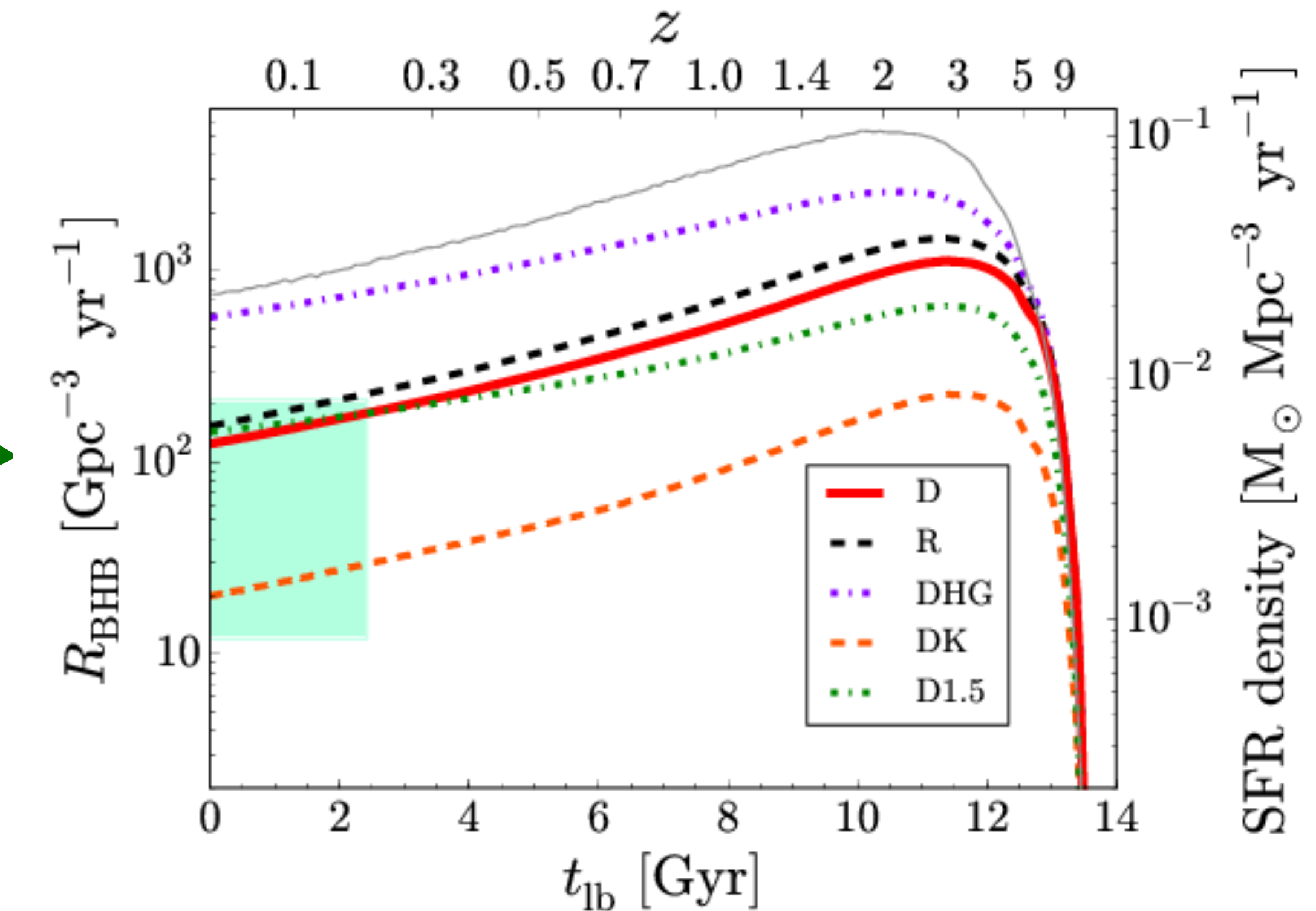


Theoretical merger rate density

Merger rate density evaluated combining **cosmological simulations** with catalogs of merging compact binaries ([Mapelli et al. 2017](#); [Schneider et al. 2017](#); [Mapelli & Giacobbo 2018](#); [Artale et al. 2020a](#))

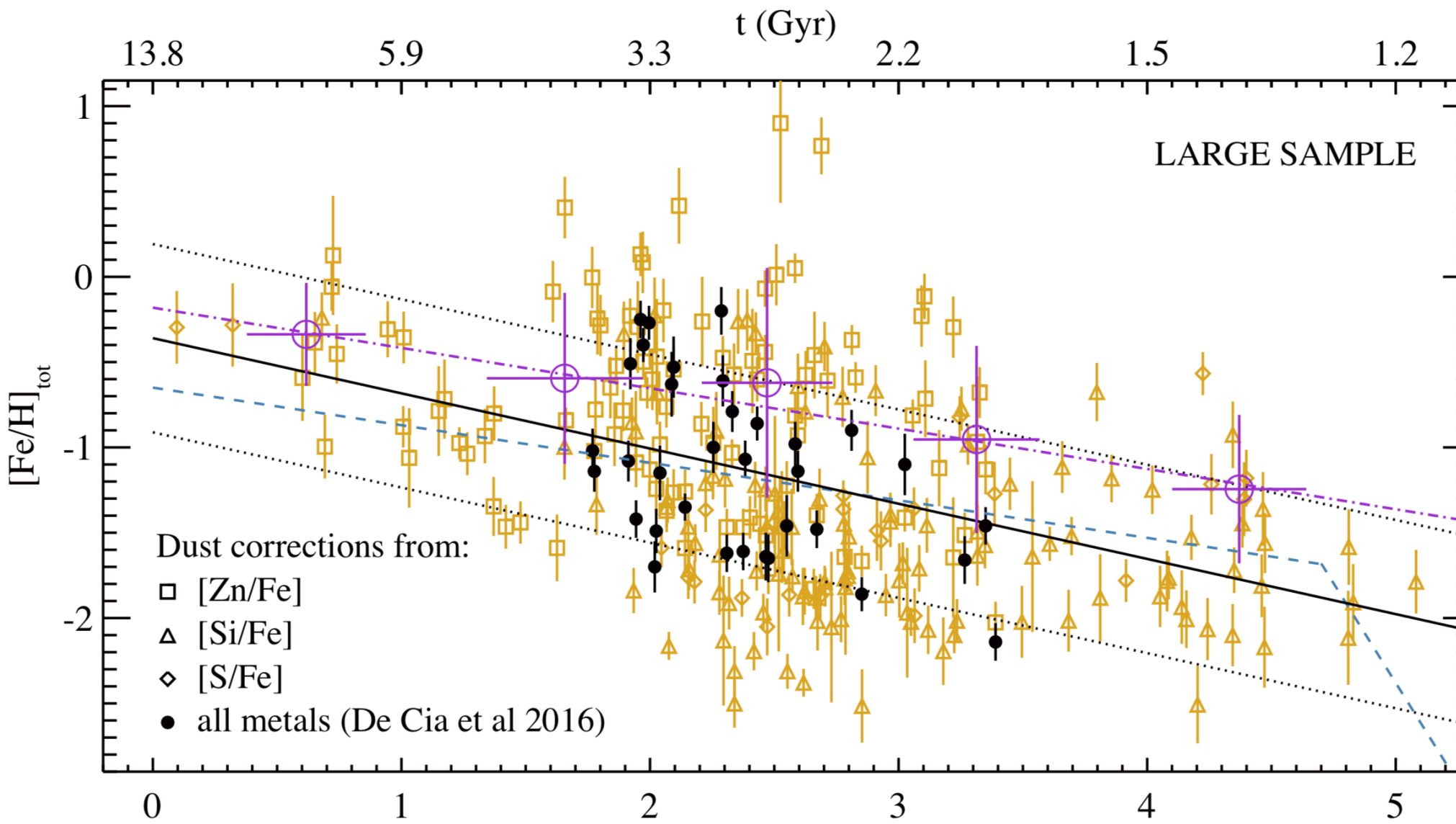
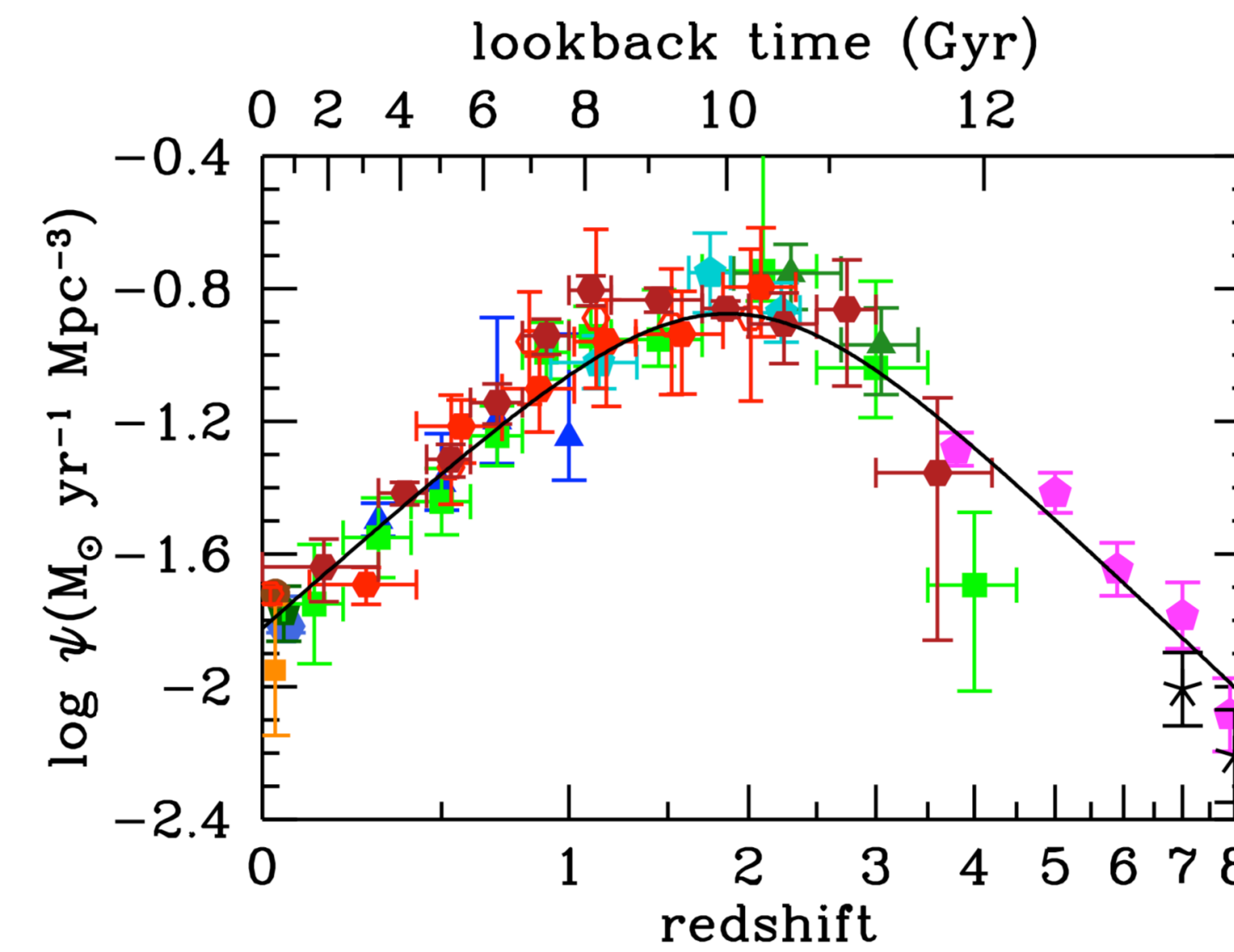
- Here an example from [Mapelli et al. 2017](#) where the **ILLUSTRIS** cosmological simulation was used.

Cosmological simulation are very expensive to run: we implemented a **semi-analytic model** ([Dominik et al. 2013](#); [Belczynski et al. 2016](#); [Eldridge & Stanway 2016](#); [Boco et al. 2019](#); [Neijssel et al. 2019](#);) which allows us to better explore the **parameter space**



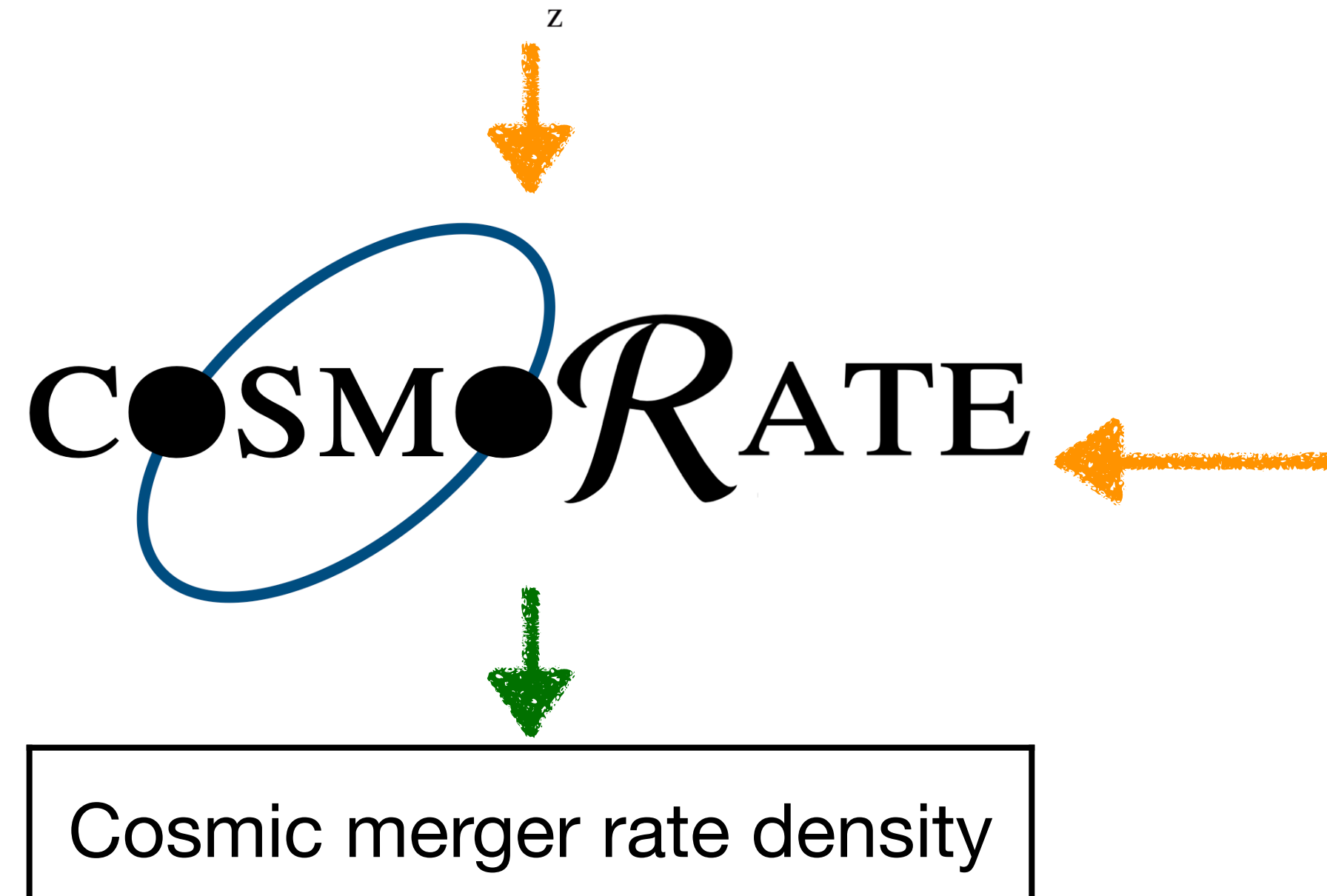
Semi-analytic model

Madau & Fragos, 2017



De Cia et al. 2018,
Gallazzi et al. 2008

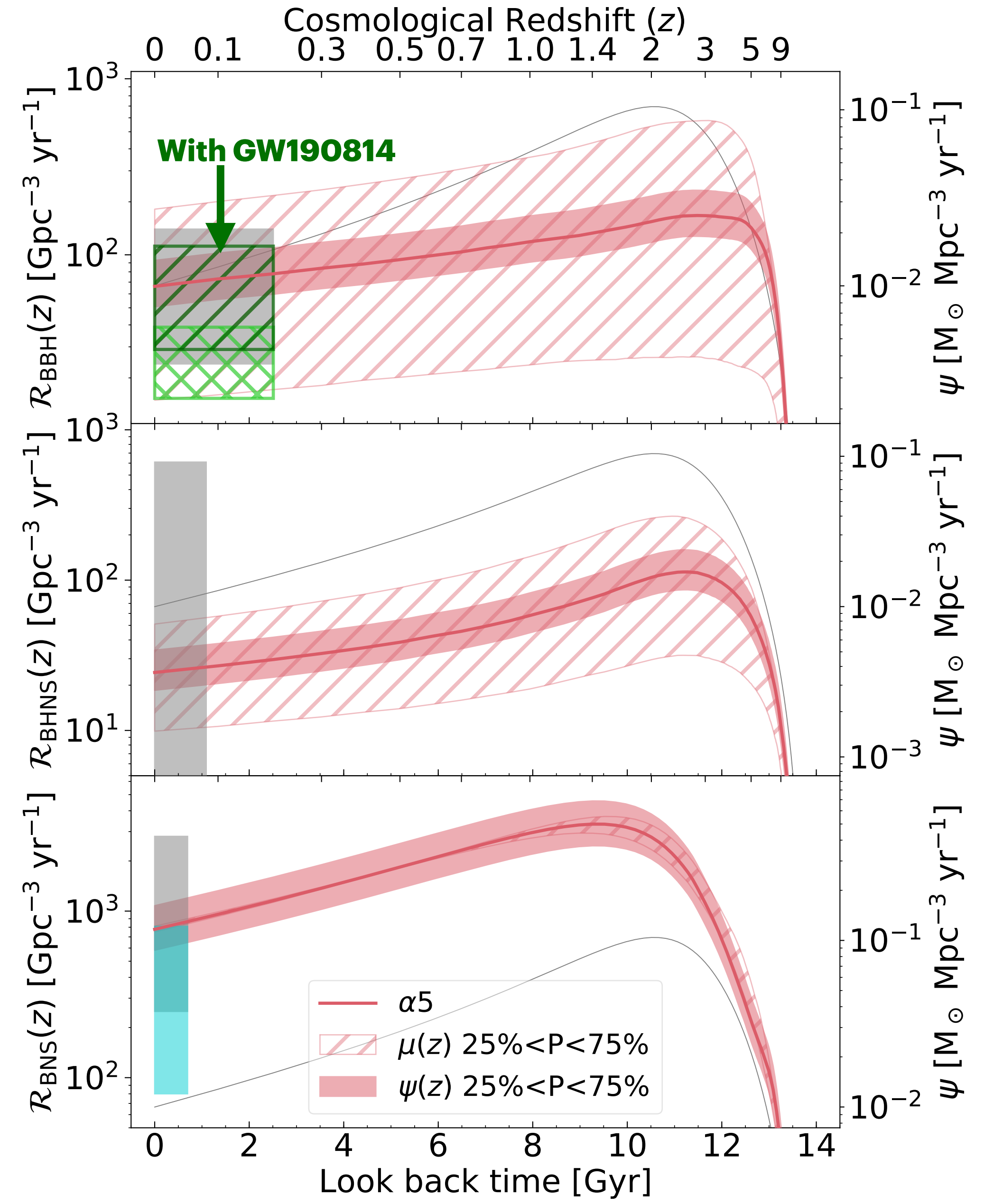
We assume a gaussian distribution around linear fit (purple line) with $\sigma = 0.5$ dex. We explored the impact of this parameter



Giacobbo and Mapelli,
2018, Di Carlo et al. 2020
and Rastello et al. 2020

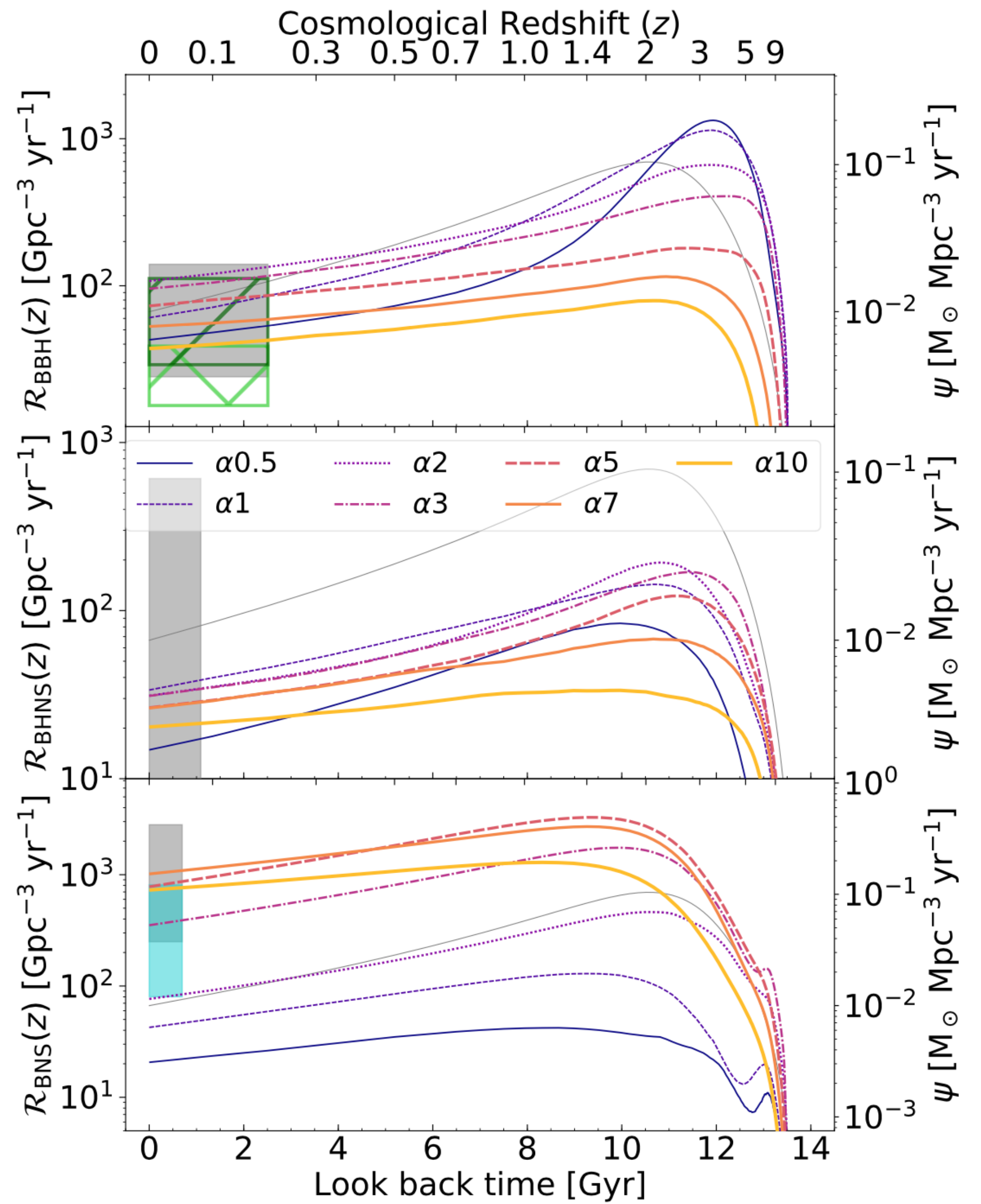
Result: impact of observational uncertainty

- Here we show an estimation of the **uncertainty** given by observed **cosmological** quantities
- $R_{\text{BBH}}(z)$ and $R_{\text{BHNS}}(z)$ are **heavily affected** by uncertainties on **metallicity** evolution.
- In contrast, the uncertainty on $R_{\text{BNS}}(z)$ is much smaller and is **dominated** by the **SFR**.



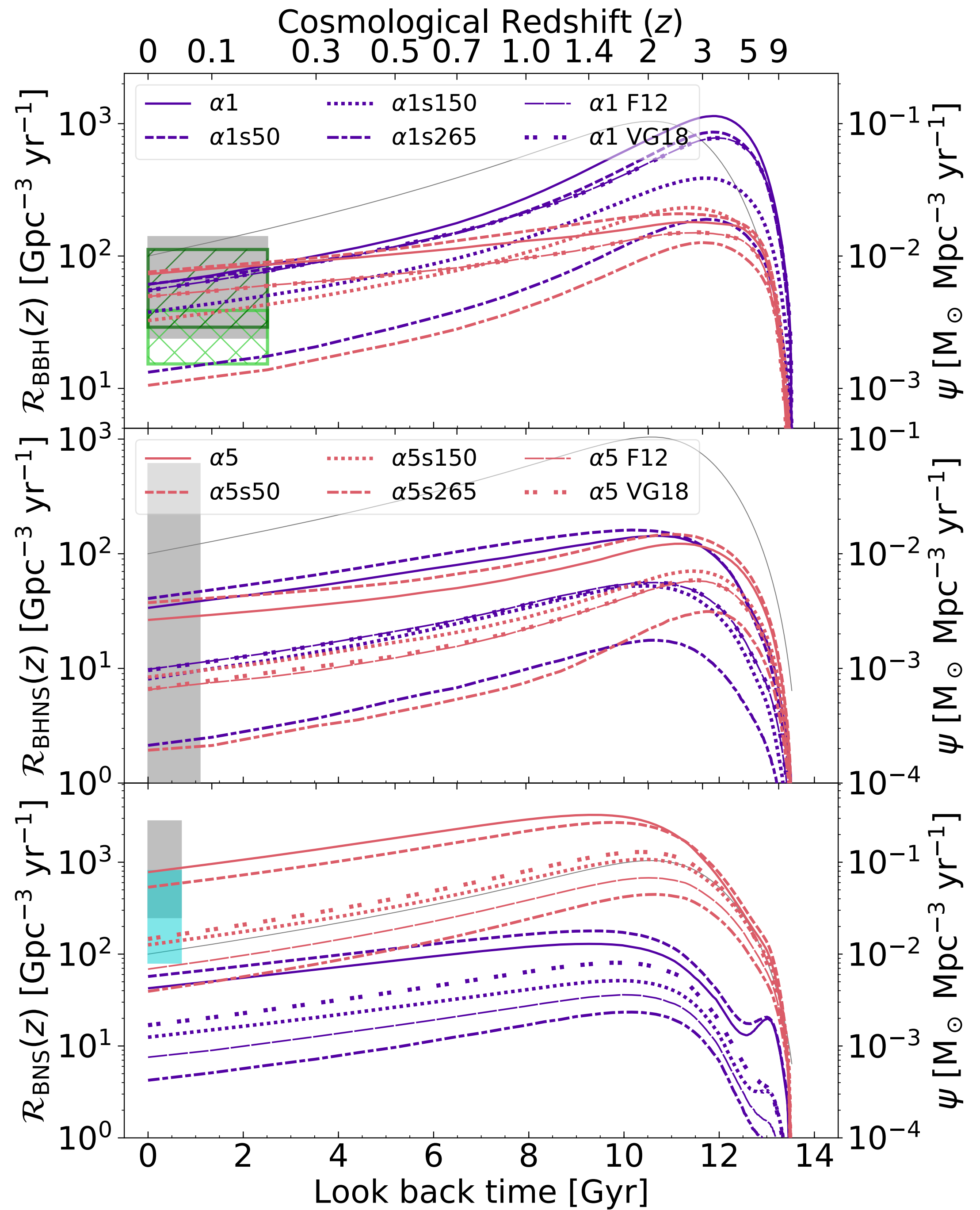
Result: common envelope parameter impact

- We **explored the parameter space** with the isolated formation channel
- The BNS merger rate density is up to **two orders of magnitude** higher for large values of α_{CE} than for low values.
- In the local Universe, $R_{\text{BBH}}(z)$ changes by a **factor of 2–3** if we vary α_{CE} .

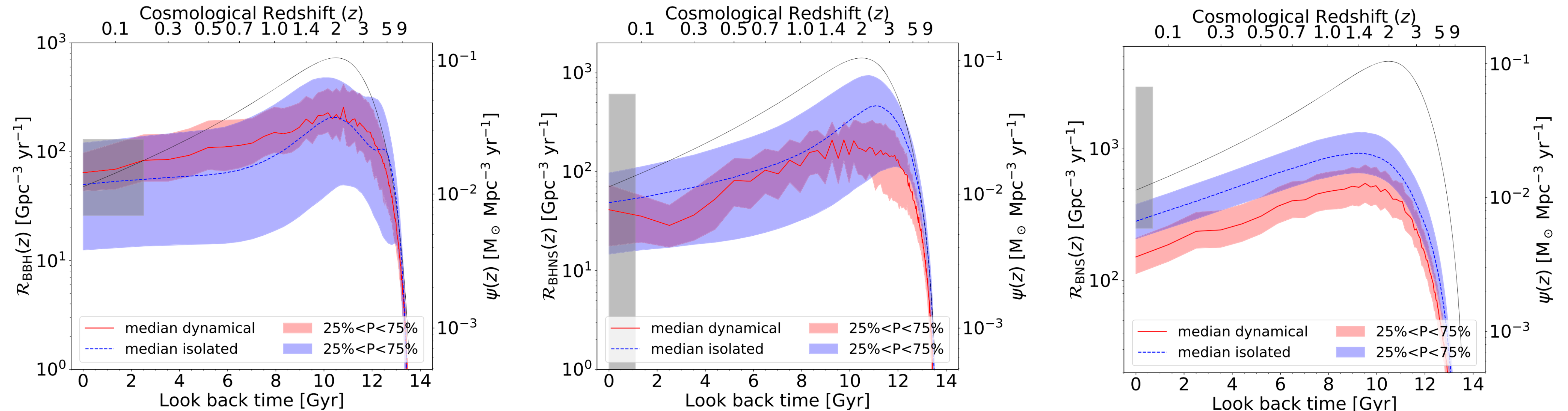


Result: natal kicks

- The effect of different SN natal kick prescriptions is higher for BNSs, where there is a difference up to an **order of magnitude** if we consider natal kicks drawn from a simple Maxwellian with $\sigma = 265 \text{ km s}^{-1}$ with respect to $\sigma = 50 \text{ km s}^{-1}$
- Only models with **relative low natal kicks** and large values of a_{CE} (like α_5 , α_5s50 , α_5s150 , and α_5VG18) are inside the 90% credible interval of GWTC-2



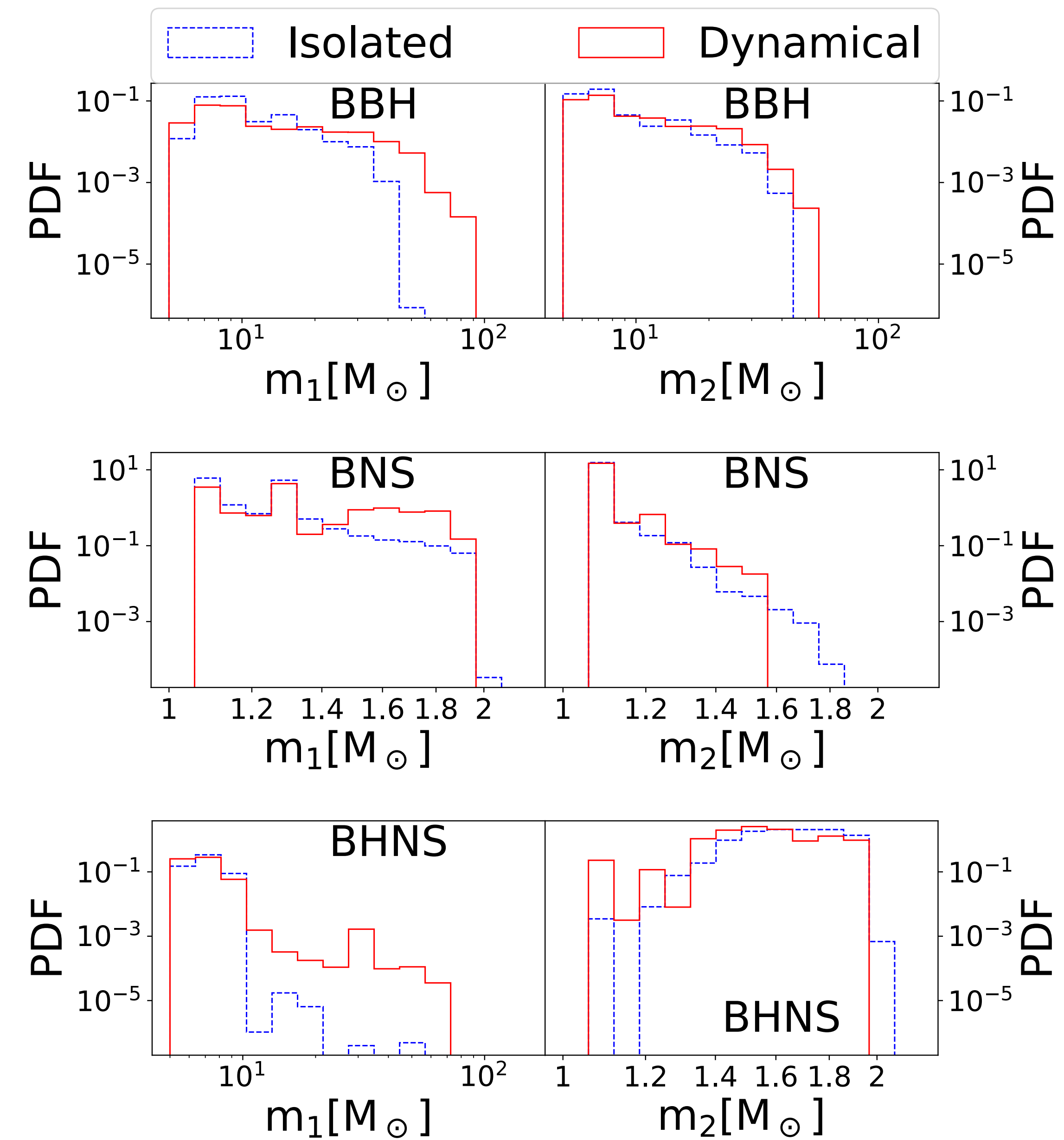
Result: different formation channels



- The **dynamical BBH merger rate is higher** than the isolated BBH merger rate between $z = 0$ and $z \sim 4$
- The MRD of dynamical BHNSs is always consistent with that of isolated BHNSs, within the estimated uncertainties
- The MRD of **dynamical BNSs** is a **factor of ~2 lower** than that of isolated BNSs, as dynamics suppress the formation of relatively low-mass binaries.

Population of merging compact binaries

- We can extract at each **redshift** a **population of compact binaries**, described by several parameters: masses, for instance
- Here, we **plot together binaries merging at different redshift** because there is no significant dependence of the mass distribution on the merger redshift, consistent with [Mapelli et al. \(2019\)](#).
- In **young star clusters**, black holes with masses $> 45 M_{\odot}$ are able to merge



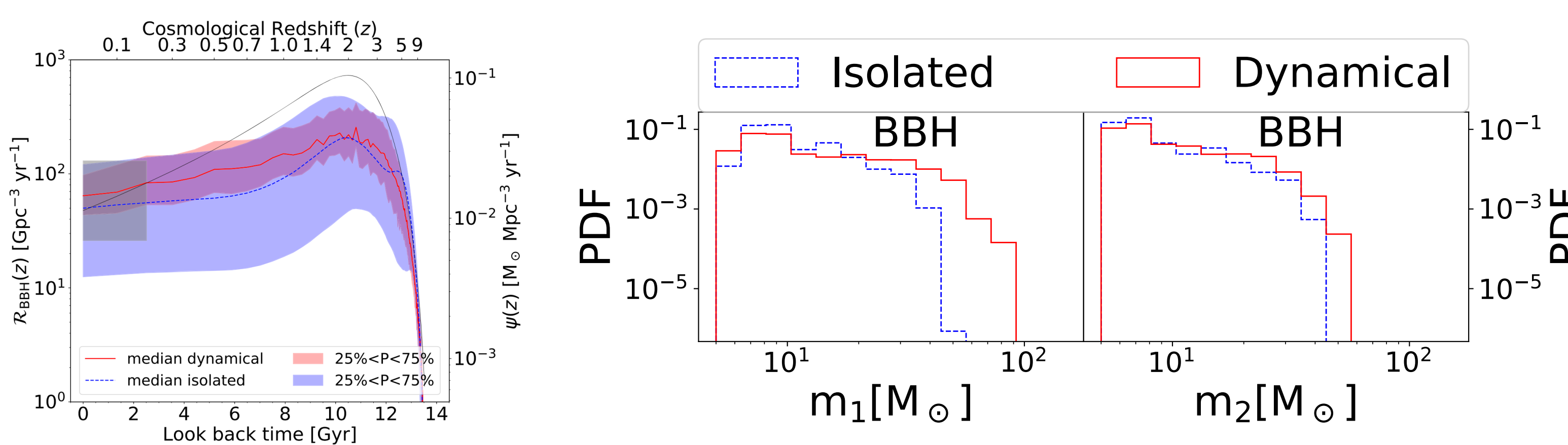
Comparison with observed population

[Bouffanais et al. 2020](#)

Theoretical Mass distribution
Theoretical Spin distribution
Cosmic merger rate density



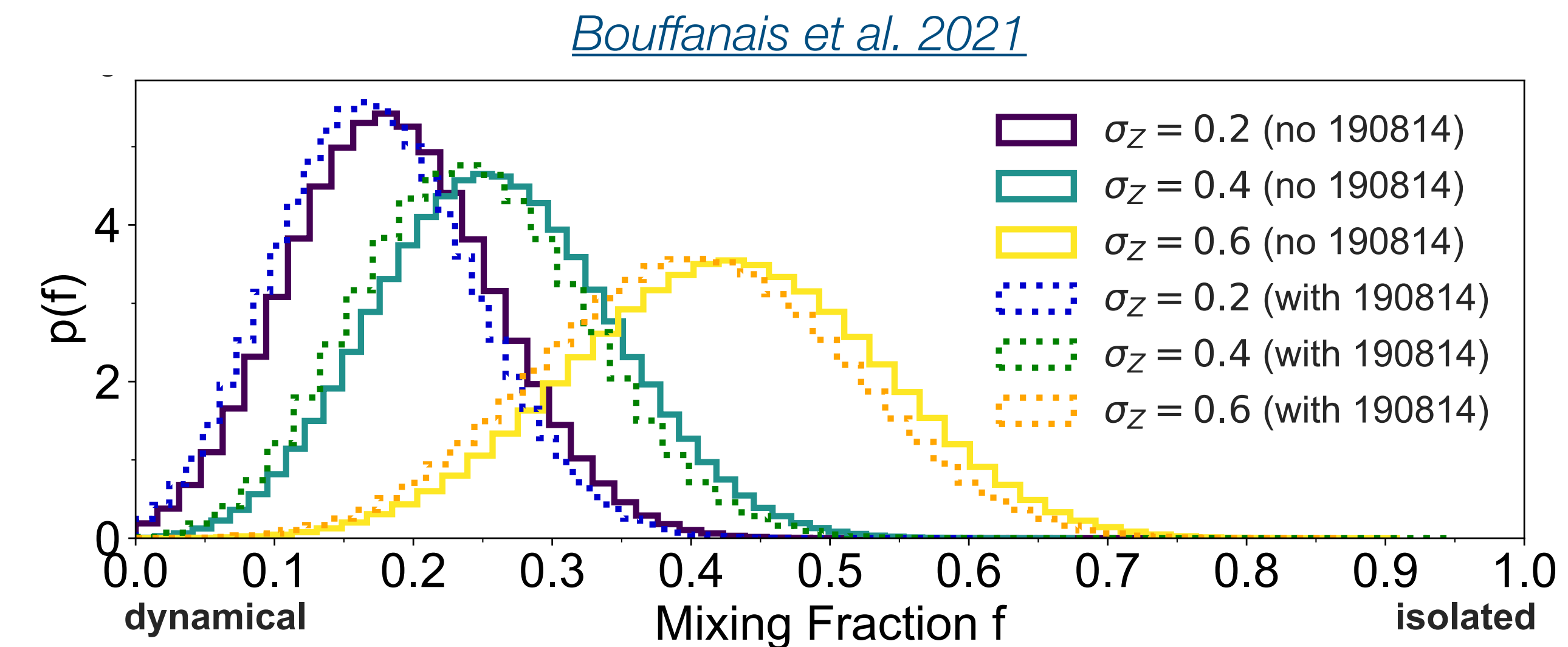
Bayesian hierarchical model
(Where you take in account detected events and selection effects)



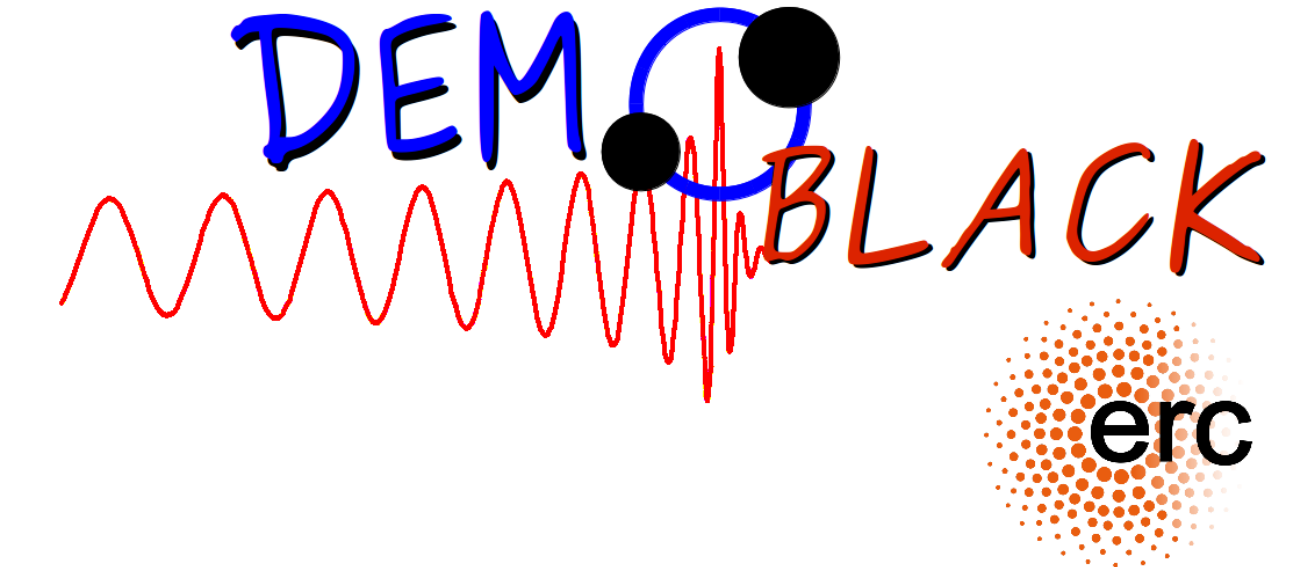
Posterior probability of key parameters, for example, a_{CE} or mixing fraction

Mixing Fraction

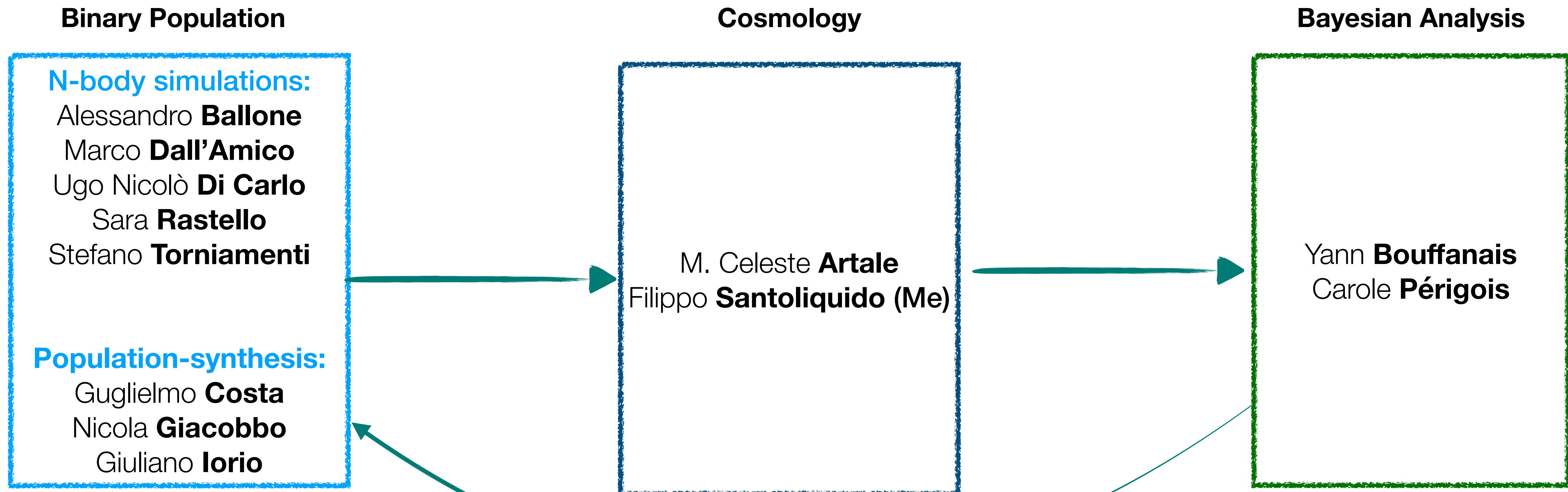
- The *mixing fraction* is the fraction of BBHs formed in young star clusters ($f=0$) versus isolated binaries ($f=1$)
- The **metallicity spread σ** plays a significant role. Assuming a large (*small*) metallicity spread tends to favour the isolated (*dynamical*) channel versus the dynamical (*isolated*).
- We find that the isolated binary evolution scenario **struggles to match all the events** listed in the GW catalogue.
- Key fact: **more than one formation channel is needed** to explain the properties of BBHs, and the dynamical path is *essential to account for the largest masses*.



The entire assembly chain:



Michela **Mapelli** is the PI



(www.demoblack.com)

Conclusions

- The number of GW detections rapidly increases and thus the astrophysical interpretation of these results is now needed more than ever before
- I developed a model that evaluates the cosmic merger rate density starting from a population of compact binaries.
- We have seen that details on binary evolution and cosmological quantities yield a great amount of uncertainty ([*Santoliquido et al. 2021*](#))
- Only models assuming values of $\alpha_{CE} > 2$ and moderately low natal kicks result in a local BNS merger rate density within the 90% credible interval inferred from the GWTC-2 ([*Abbott et al. 2021b*](#))
- We also evaluate the merger rate density for the dynamical formation channel, and we found that dynamical binary black holes are much less sensitive to metallicity than isolated ones ([*Santoliquido et al. 2020*](#)).

*Thanks a lot for the attention!
I'm happy to take your questions*

You can always write me at filippo.santoliquido@phd.unipd.it

Back up slides

Inferred population properties

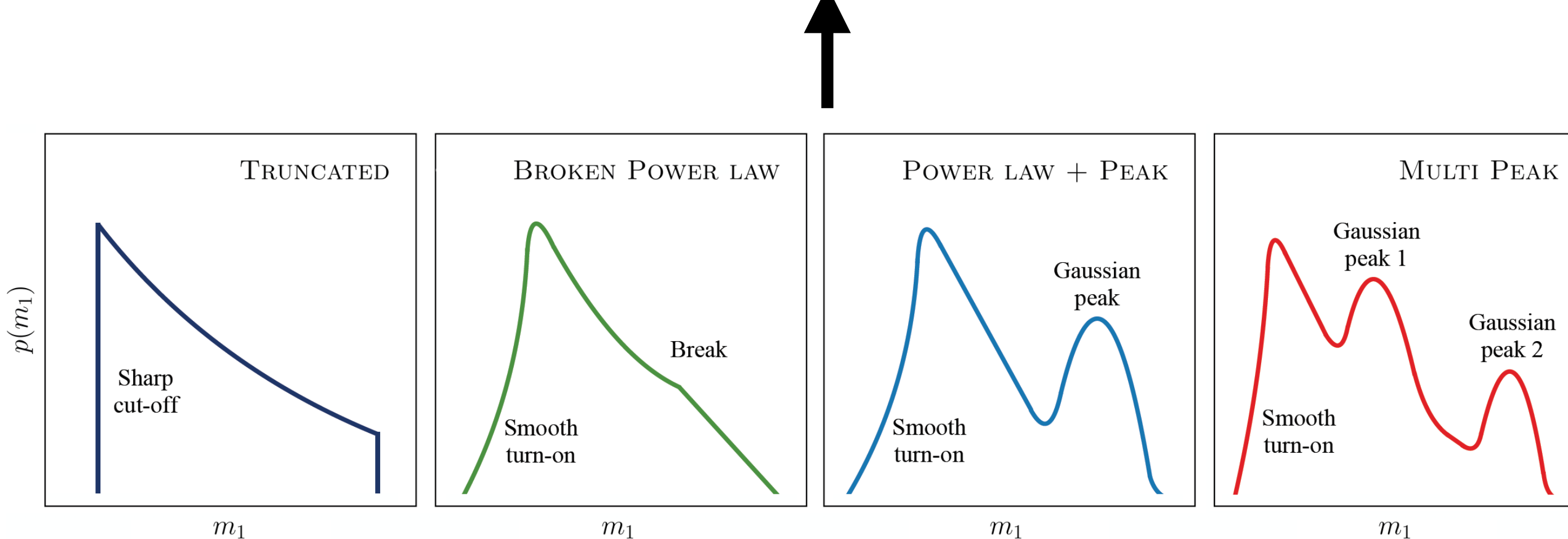
Set of initial Assumption

Mass distribution shape
Spin distribution shape
merger rate density with redshift trend



Bayesian hierarchical model

(Where you take in account detected events and selection effects)



Posterior probability of the inferred population properties
Among which the **merger rate density**

Abbott et al. 2021b, <https://arxiv.org/abs/2010.14533>

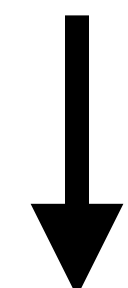
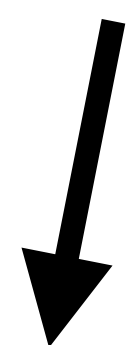
Bayesian hierarchical model

- Loredo 2004; Mandel et al. 2019; Thrane & Talbot 2019

$$\mathcal{L}(\{d\} | \Lambda, N) \propto N^{N_{\text{det}}} e^{-N\xi(\Lambda)} \prod_{i=1}^{N_{\text{det}}} \int \mathcal{L}(d_i | \theta) \pi(\theta | \Lambda) d\theta$$

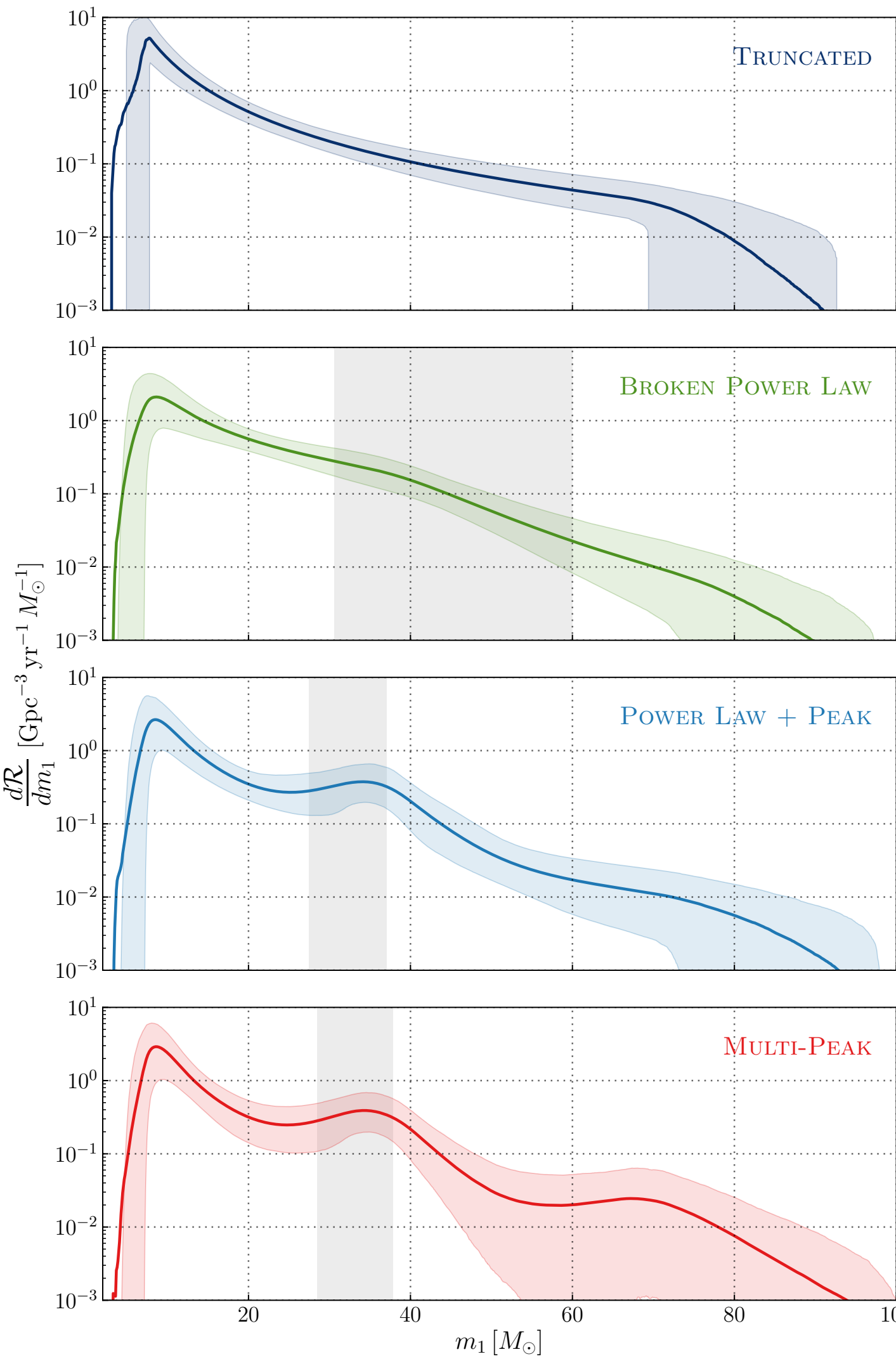
Expected number of detections

For each model associated with the hyperparameter. We evaluate the probability to detect each binary system evaluating its waveform and considering the current gravitational wave network ad design sensitivity



Integrals for the i-th GW observations
 θ are the parameters that describe the observations:
for example, chirp mass, mass ratio and merging redshift

Astrophysical sources



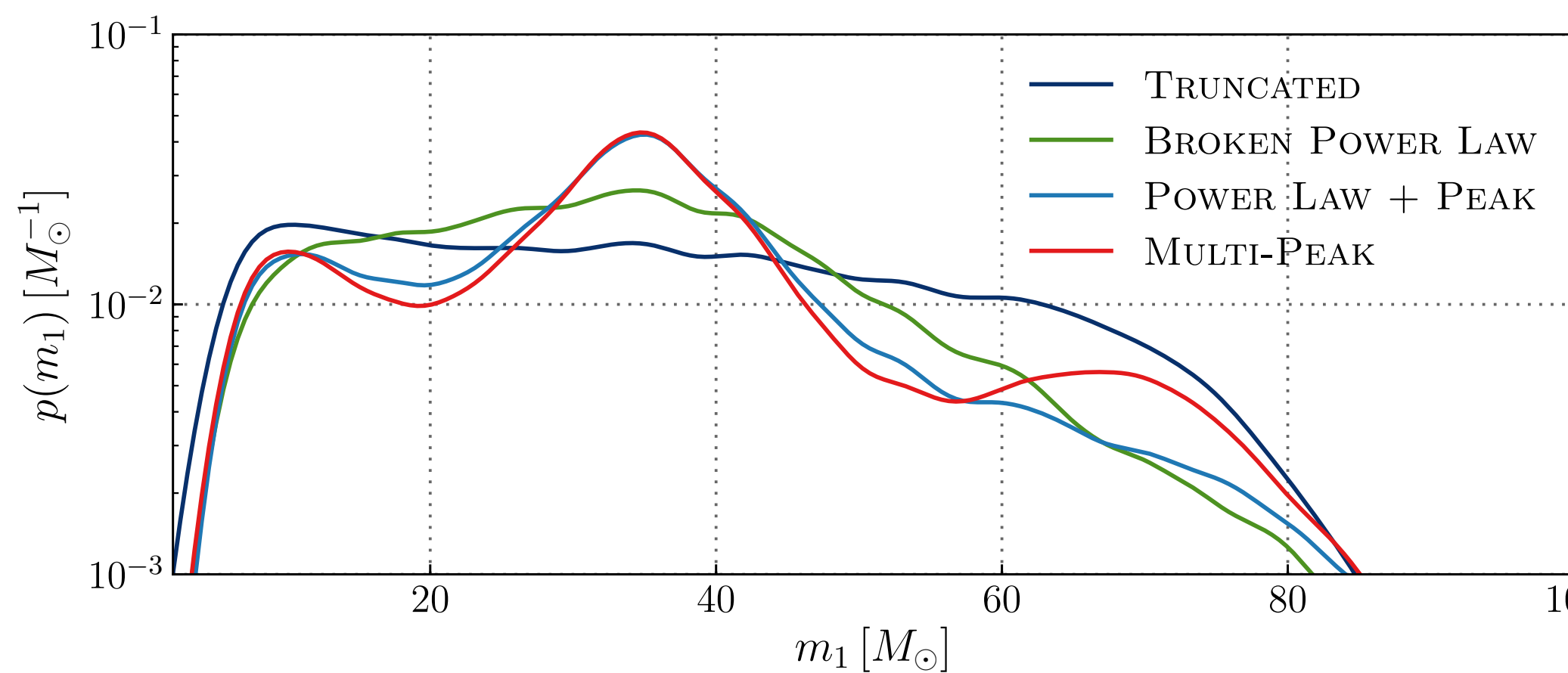
The mass distribution

Mass model	\mathcal{B}	$\log_{10} \mathcal{B}$
POWER LAW + PEAK	1.0	0.0
MULTI PEAK	0.5	-0.3
BROKEN POWER LAW	0.12	-0.92
TRUNCATED	0.01	-1.91

Bayes factor

$$\mathcal{R}_{\text{BBH}} = 23.9^{+14.9}_{-8.6} \text{ Gpc}^{-3} \text{ yr}^{-1}$$

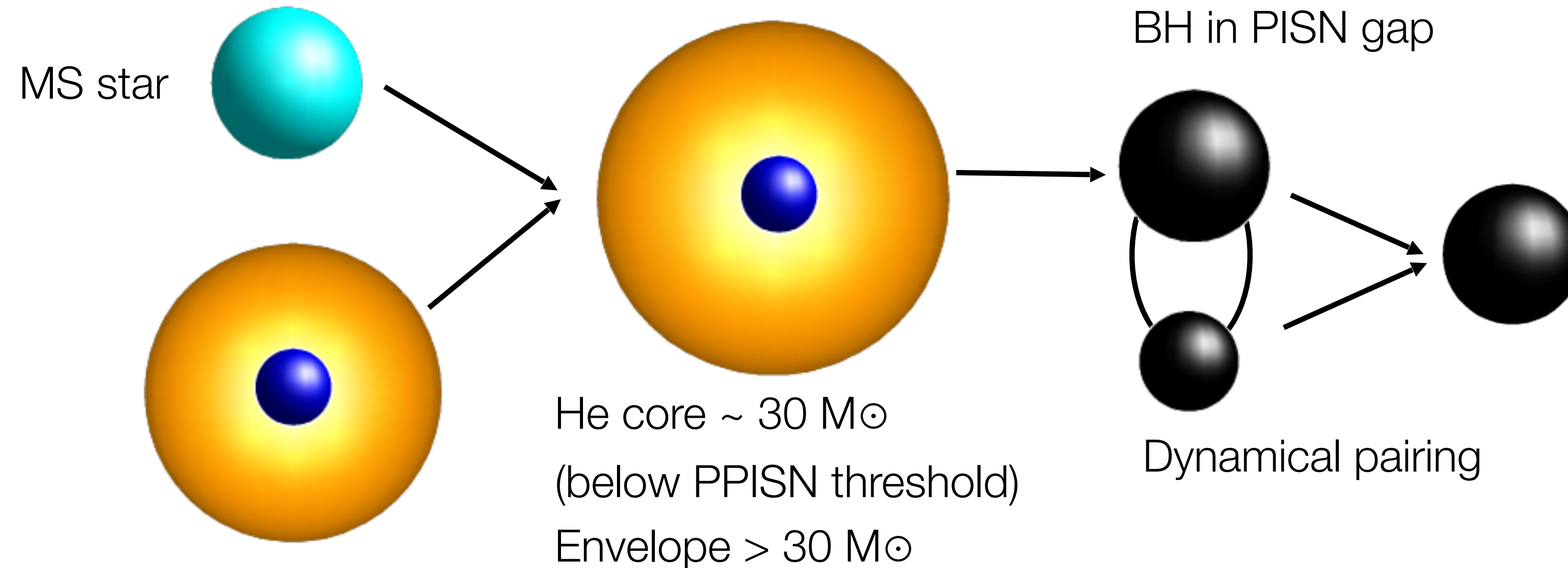
Power Law + Peak



Observed mass distribution

Abbott et al. 2021b, <https://arxiv.org/abs/2010.14533>

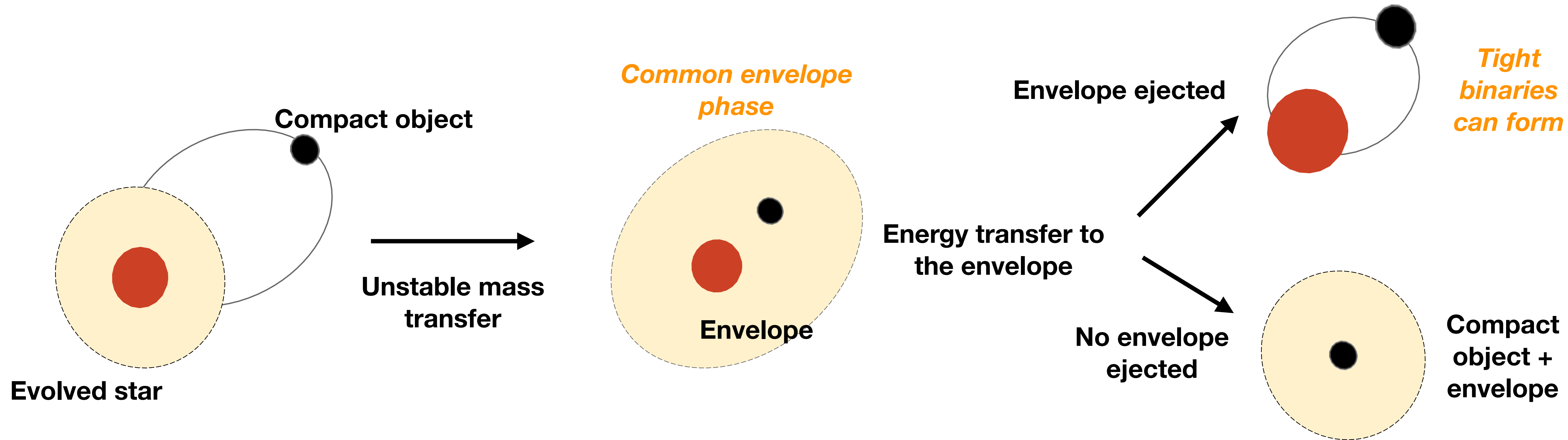
How can we form BBH in the pair instability mass gap in the dynamical formation channel?



[Di Carlo et al. 2019, MNRAS 487, 4947](#)

[Di Carlo et al. 2020a, MNRAS, 497, 1043](#)

Details on common envelope phase



$\alpha\lambda$ -formalism [Webbink 1984](#)

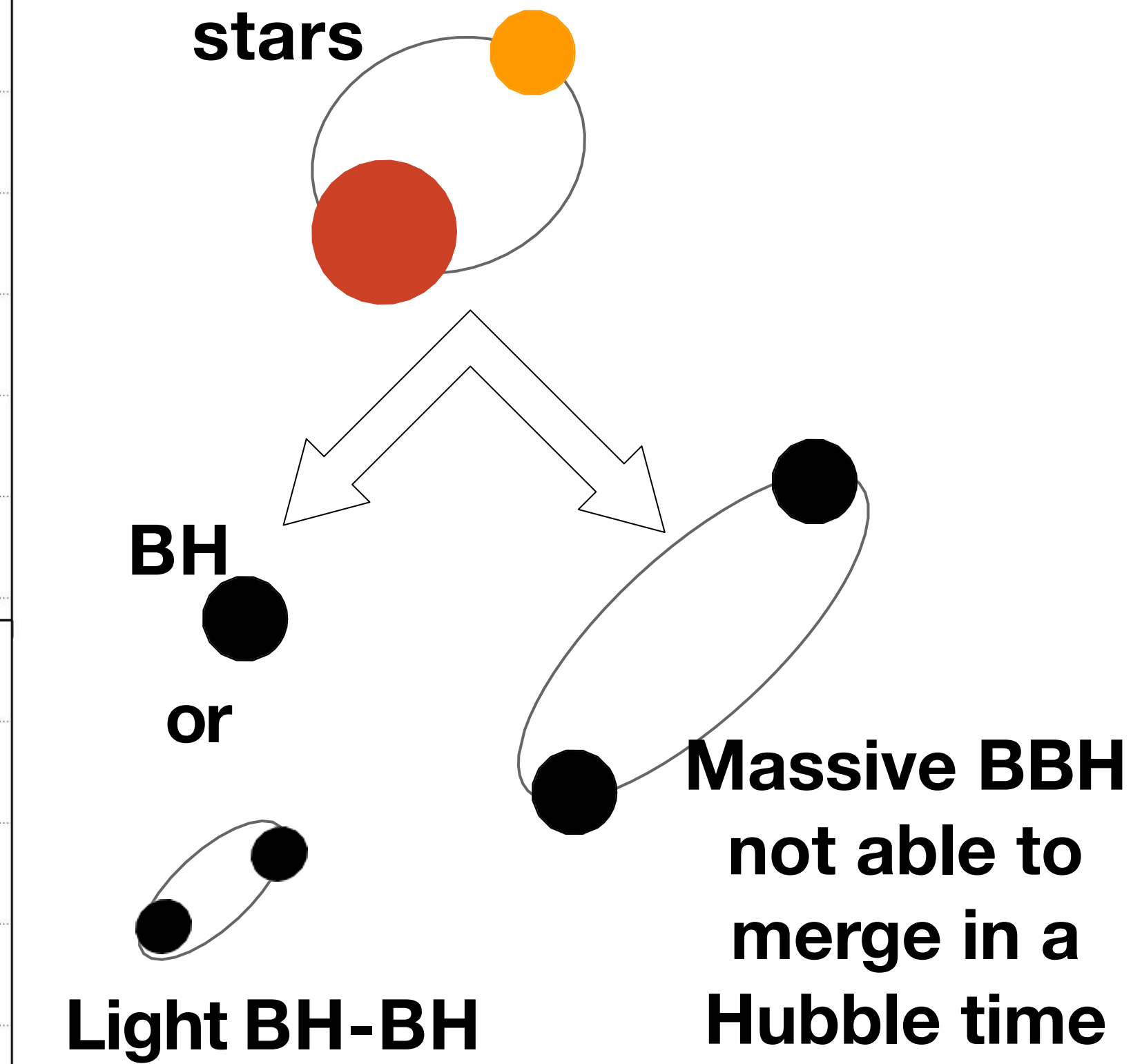
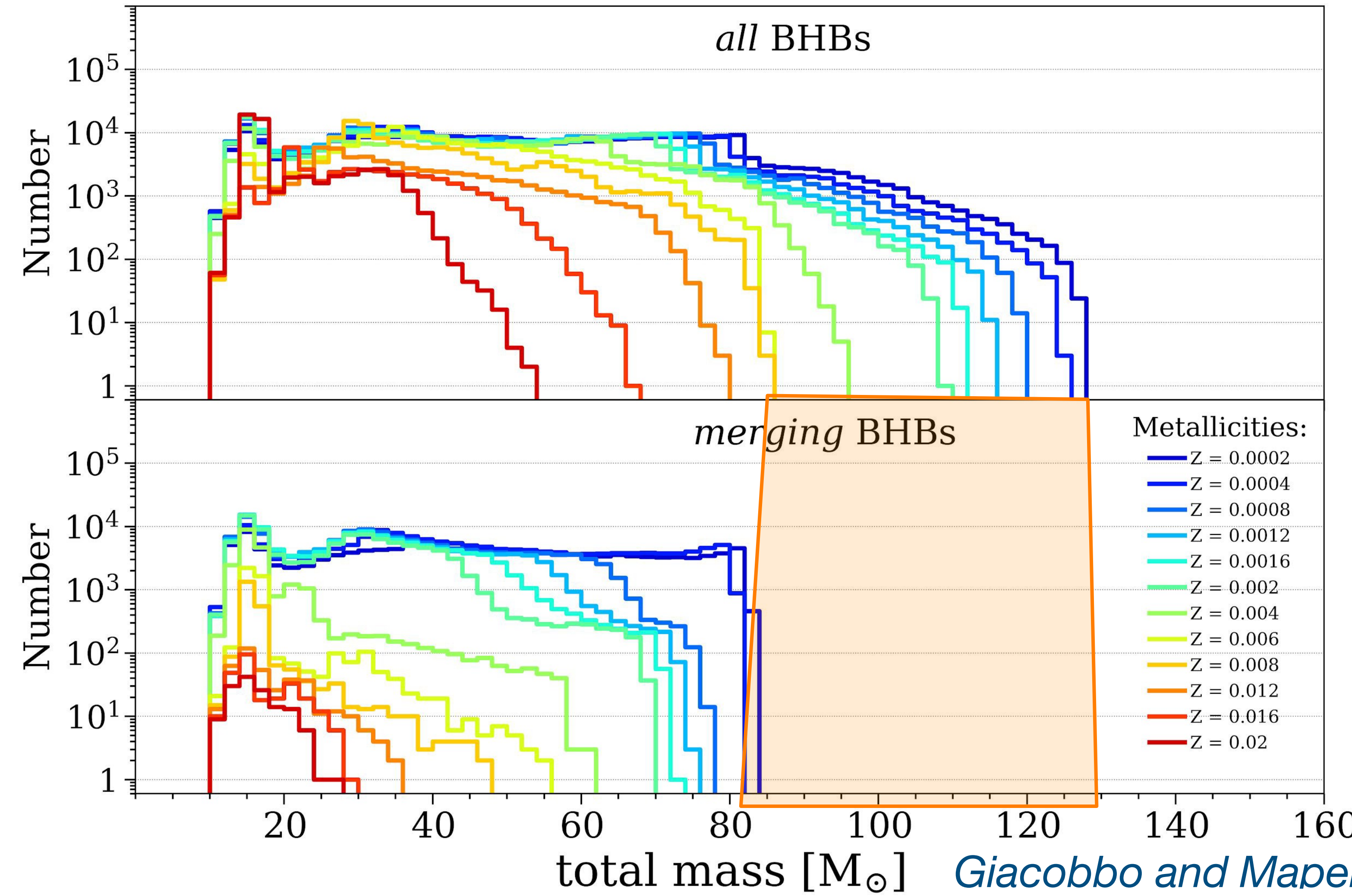
Transfer efficiency of orbital energy to the common envelope

$$\alpha \left(-\frac{Gm_1m_2}{2a_{ini}} + G\frac{m_{1,core}m_2}{2a_{fin}} \right) = \frac{m_1m_{1,env}}{R_1\lambda}$$

Describes the binding energy of the common envelope

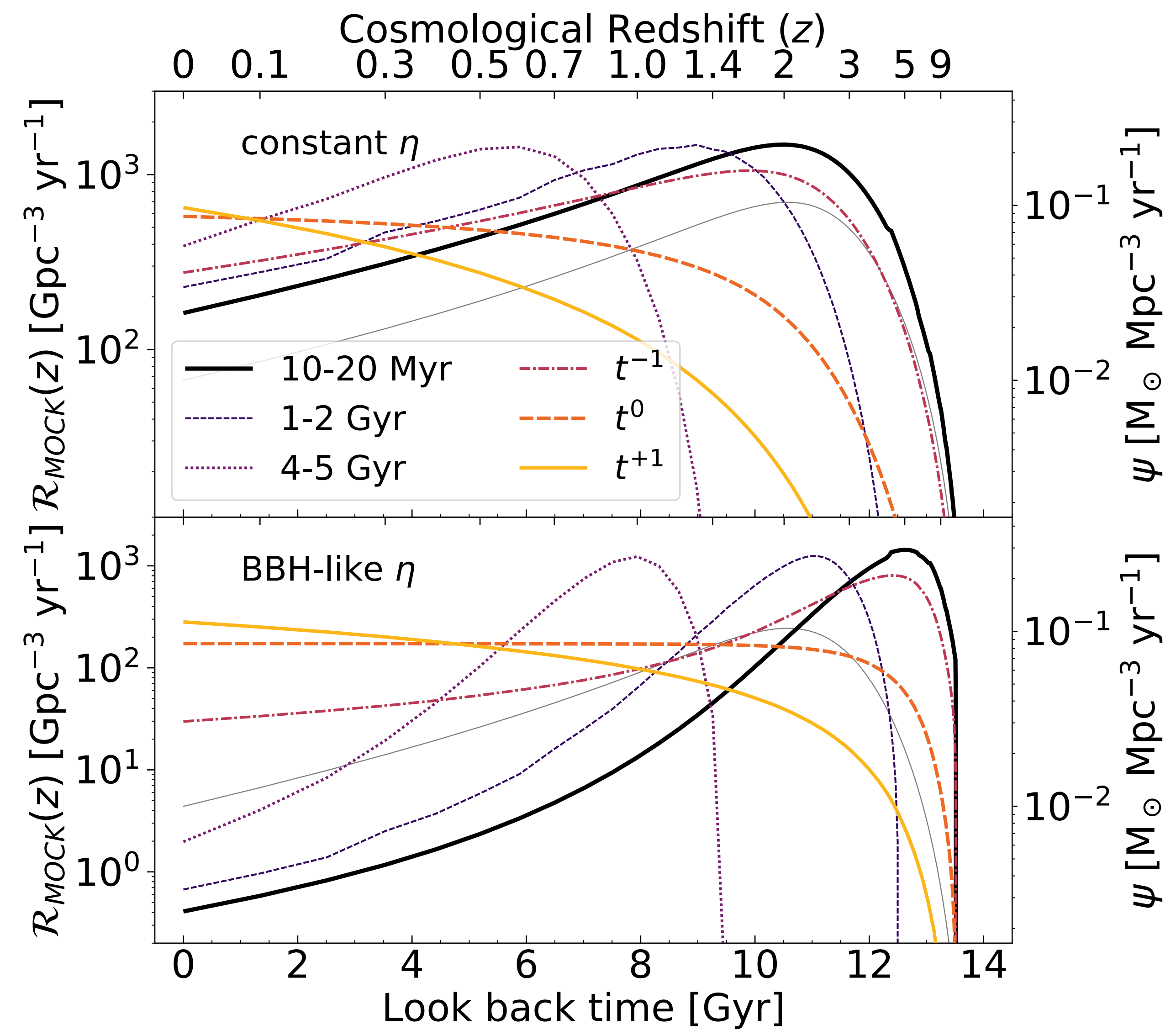
Impact of metallicity on mass distribution

From $\sim 2 \times 10^8$ systems



Mock catalogues

- **Constant η :** if the delay time is uniformly distributed between 10 and 20 Myr, the merger rate density has exactly the same slope and peak redshift as the cosmic SFR. The other two narrow delay time distributions have the effect to shift the merger rate density peak towards lower redshifts than the peak of the cosmic SFR
- **BBH-like η :** The delay time distribution uniform between 10 and 20 Myr peaks at a higher redshift ($z > \sim 5$) with respect to the cosmic SFR density.



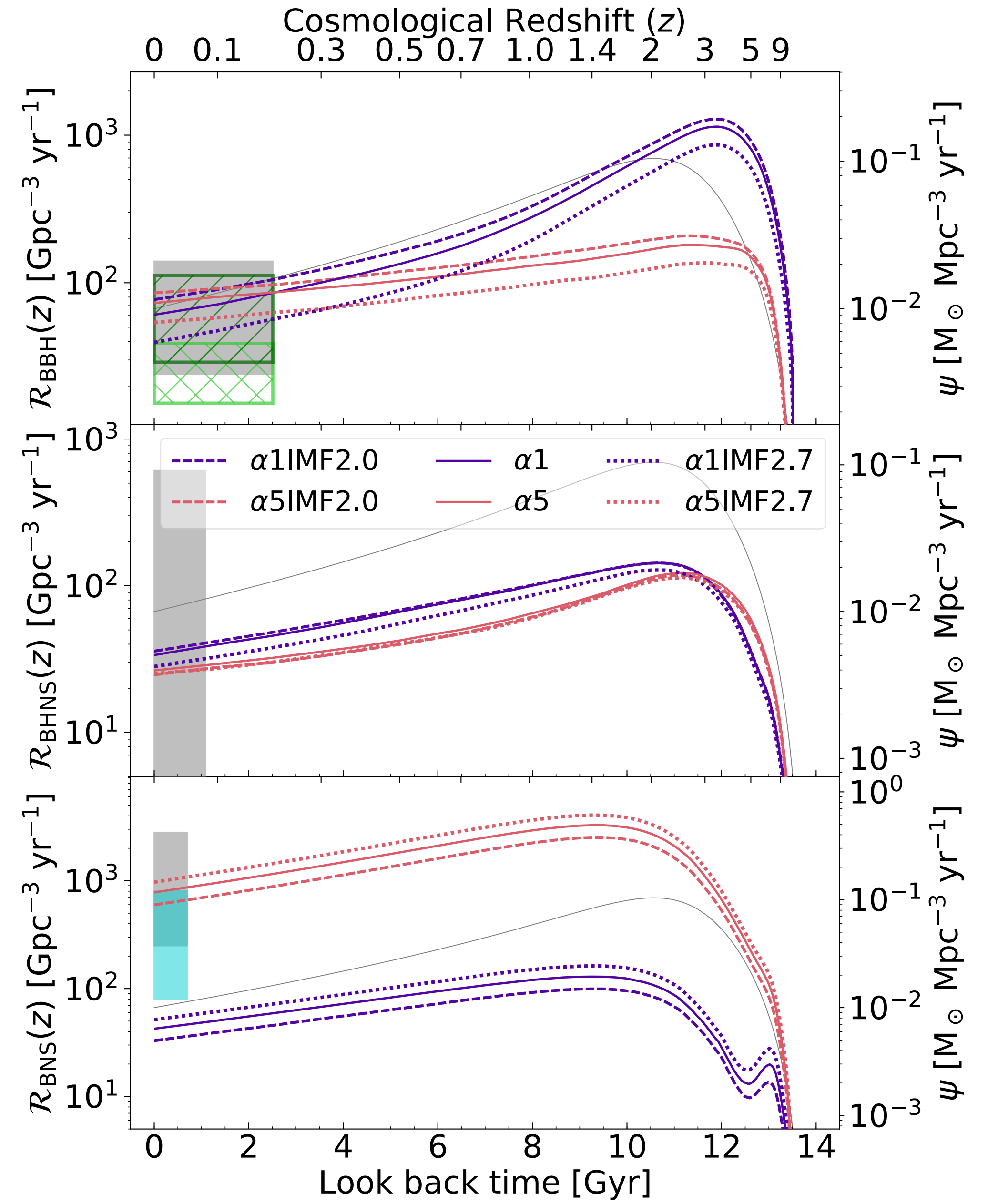
Summary of the models considered in Santoliquido+2021

Model Name	α_{CE}	Kick Model	SN Model	f_{MT}	α_{IMF}
$\alpha 0.5$	0.5	Eq. 2	Delayed	H02	2.3
$\alpha 1$	1	Eq. 2	Delayed	H02	2.3
$\alpha 2$	2	Eq. 2	Delayed	H02	2.3
$\alpha 3$	3	Eq. 2	Delayed	H02	2.3
$\alpha 5$	5	Eq. 2	Delayed	H02	2.3
$\alpha 7$	7	Eq. 2	Delayed	H02	2.3
$\alpha 10$	10	Eq. 2	Delayed	H02	2.3
$\alpha 1s265$	1	$\sigma_{1D} = 265 \text{ km/s}$	Delayed	H02	2.3
$\alpha 5s265$	5	$\sigma_{1D} = 265 \text{ km/s}$	Delayed	H02	2.3
$\alpha 1s150$	1	$\sigma_{1D} = 150 \text{ km/s}$	Delayed	H02	2.3
$\alpha 5s150$	5	$\sigma_{1D} = 150 \text{ km/s}$	Delayed	H02	2.3
$\alpha 1s50$	1	$\sigma_{1D} = 50 \text{ km/s}$	Delayed	H02	2.3
$\alpha 5s50$	5	$\sigma_{1D} = 50 \text{ km/s}$	Delayed	H02	2.3
$\alpha 1F12$	1	Eq. 3	Delayed	H02	2.3
$\alpha 5F12$	5	Eq. 3	Delayed	H02	2.3
$\alpha 1VG18$	1	$\sigma_{\text{high}} = 265 \text{ km/s}$ $\sigma_{\text{low}} = 30 \text{ km/s}$	Delayed	H02	2.3
$\alpha 5VG18$	5	$\sigma_{\text{high}} = 265 \text{ km/s}$ $\sigma_{\text{low}} = 30 \text{ km/s}$	Delayed	H02	2.3
$\alpha 1R$	1	Eq. 2	Rapid	H02	2.3
$\alpha 5R$	5	Eq. 2	Rapid	H02	2.3
$\alpha 1MT0.1$	1	Eq. 2	Delayed	0.1	2.3
$\alpha 1MT0.5$	1	Eq. 2	Delayed	0.5	2.3
$\alpha 1MT1.0$	1	Eq. 2	Delayed	1.0	2.3
$\alpha 5MT0.1$	5	Eq. 2	Delayed	0.1	2.3
$\alpha 5MT0.5$	5	Eq. 2	Delayed	0.5	2.3
$\alpha 5MT1.0$	5	Eq. 2	Delayed	1.0	2.3
$\alpha 10MT0.1$	10	Eq. 2	Delayed	0.1	2.3
$\alpha 10MT0.5$	10	Eq. 2	Delayed	0.5	2.3
$\alpha 10MT1.0$	10	Eq. 2	Delayed	1.0	2.3
$\alpha 1IMF2.0$	1	Eq. 2	Delayed	H02	2.0
$\alpha 1IMF2.7$	1	Eq. 2	Delayed	H02	2.7
$\alpha 5IMF2.0$	5	Eq. 2	Delayed	H02	2.0
$\alpha 5IMF2.7$	5	Eq. 2	Delayed	H02	2.7

Column 1: model name. Column 2: parameter α_{CE} of the CE. Column 3: kick model; runs $\alpha 1s265/\alpha 5s265$, $\alpha 1s150/\alpha 5s150$ and $\alpha 1s50/\alpha 5s50$ have natal kicks drawn from a Maxwellian distribution with root mean square $\sigma_{1D} = 265, 150$ and 50 km s^{-1} , respectively; runs $\alpha 1F12$ and $\alpha 5F12$ adopt the natal kick model in eq. 3; runs $\alpha 1VG18$ and $\alpha 5VG18$ assume the same model as [Vigna-Gómez et al. \(2018\)](#); in all the other models, the kicks are calculated as in eq. 2. Column 4: core collapse SN model; models $\alpha 1R$ and $\alpha 5R$ adopt the rapid model from [Fryer et al. \(2012\)](#), while all the other models adopt the delayed model from the same authors. Column 5: accretion efficiency f_{MT} onto a non-degenerate accretor; H02 means that we follow the same formalism as in [Hurley et al. \(2002\)](#). For the other models, see eq. 4. Column 6: slope of the IMF; models α_{IMF} of the IMF for $m > 0.5 \text{ M}_\odot$; $\alpha 1K2.0, \alpha 5K2.0$ ($\alpha 1K2.7, \alpha 5K2.7$) have $\alpha_{\text{IMF}} = 2.0$ ($\alpha_{\text{IMF}} = 2.7$). All the other models assume the "standard" slope $\alpha_{\text{IMF}} = 2.3$ ([Kroupa 2001](#)).

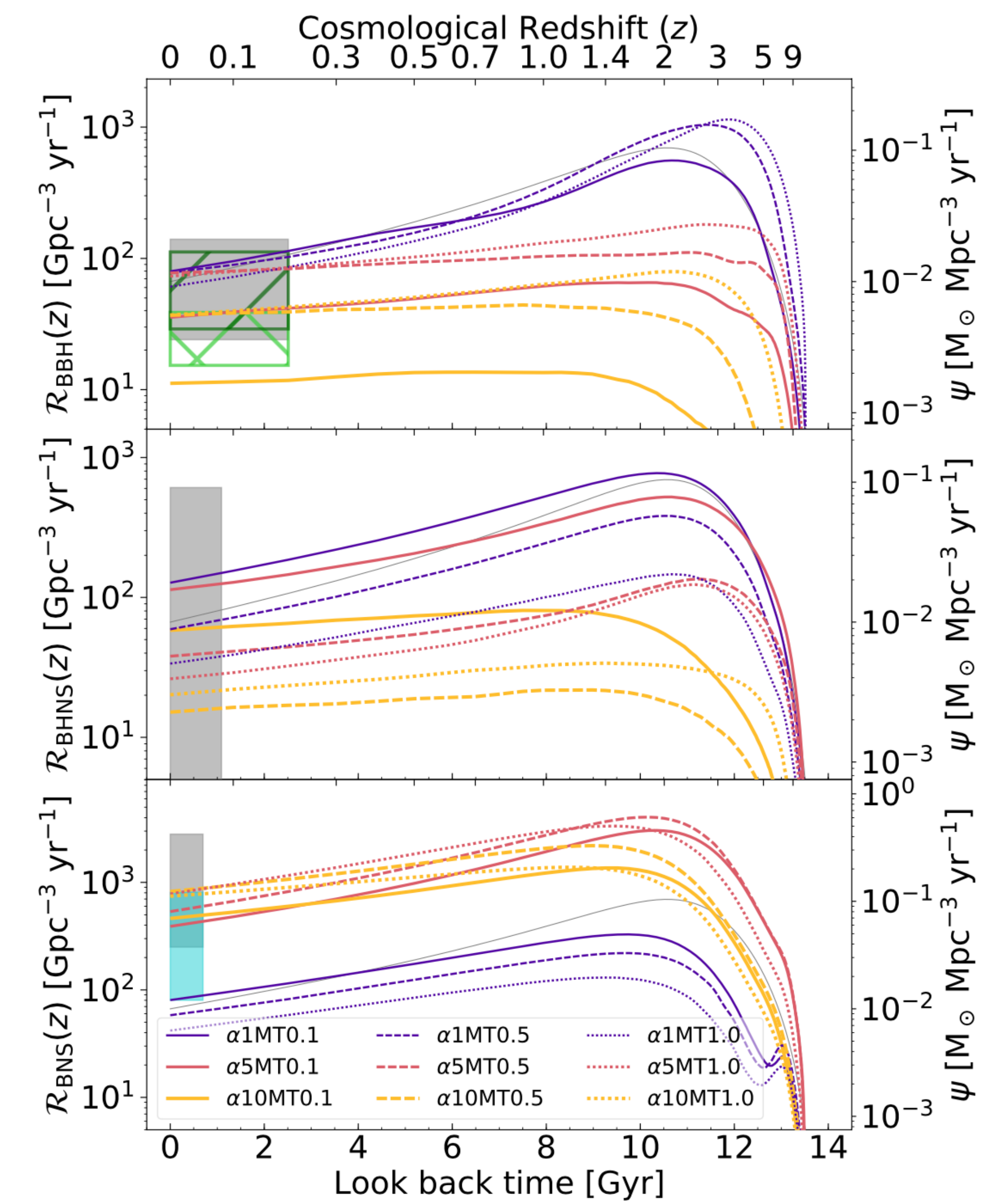
Result: impact of different initial mass function

- The figure shows that the impact of varying the IMF's slope on the cosmic merger rate is very mild, as already found by [*Klencki et al. 2018.*](#)
- $R_{\text{BBH}}(z)$ and $R_{\text{BNS}}(z)$ show an opposite trend: the former is higher when a shallower IMF slope is considered. This result has a trivial explanation: if $\alpha_{\text{IMF}} = 2.0$, the fraction of massive stars that end up collapsing into black hole is higher with respect to $\alpha_{\text{IMF}} = 2.7$.



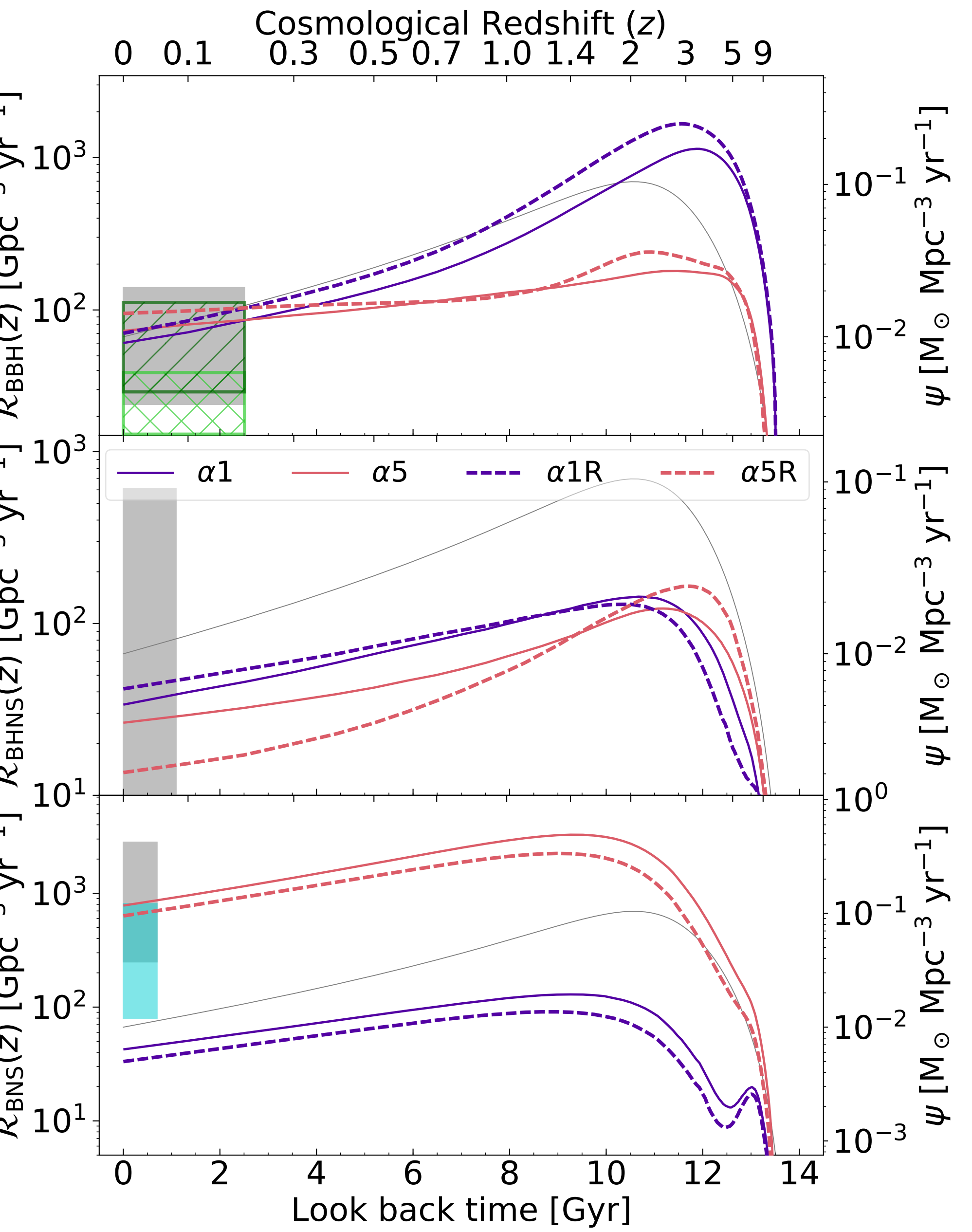
Result: mass transfer efficiency impact

- **Low mass transfer efficiency ($f_{MT} < 1$)** significantly reduces the total mass of the binary star. In the sense that, the **secondary star accretes just a small fraction** of the mass lost by the primary star during Roche lobe overflow.
- This implies that low mass transfer efficiency **enhances the formation** of unequal mass binary compact objects, such as **BHNSs**.



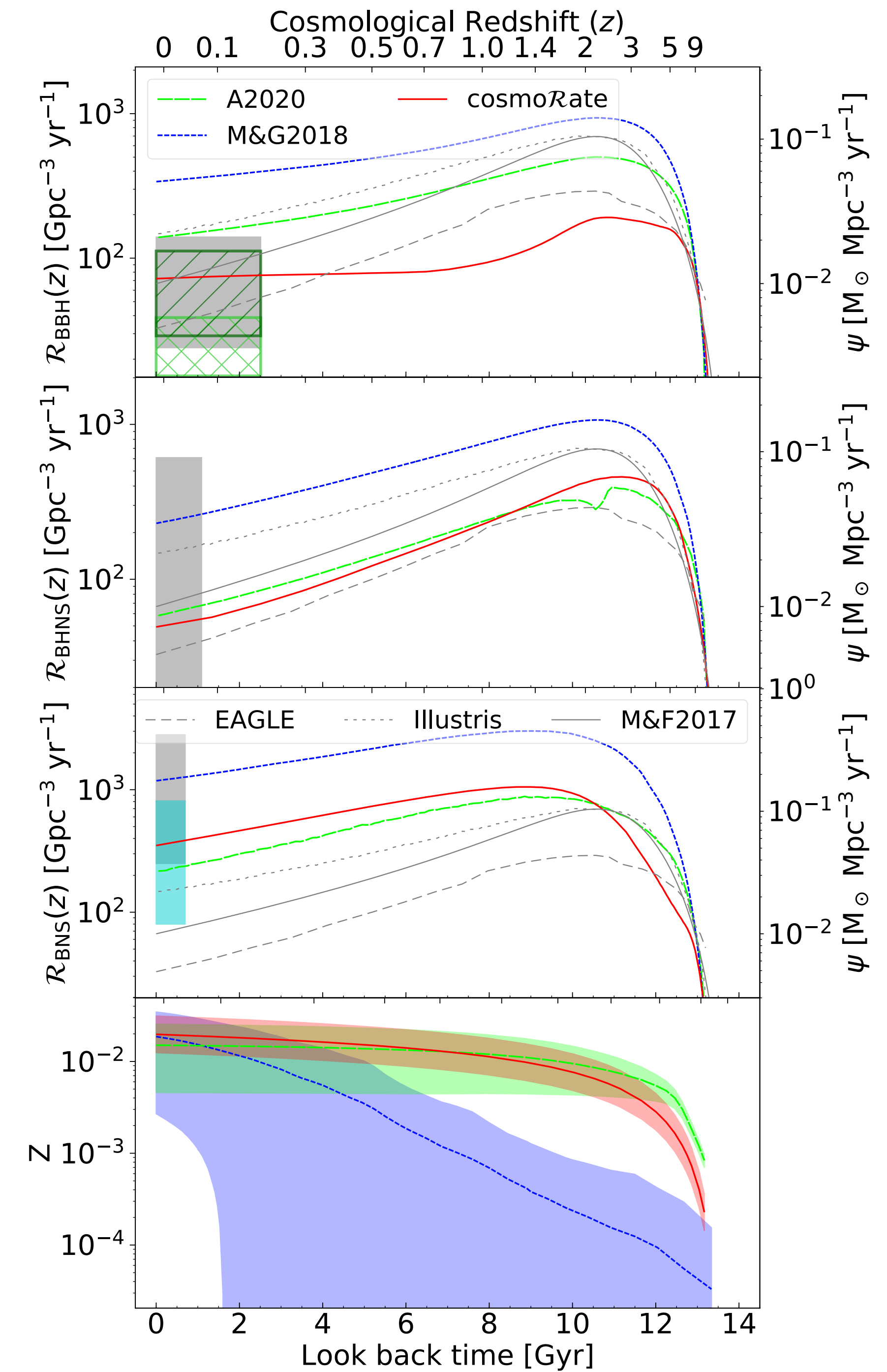
Result: SN model

- The delayed model slightly enhances $R_{\text{BNS}}(z)$, because it produces more massive neutron stars which can merge on a shorter timescale. For the same reason, the delayed model slightly suppresses $R_{\text{BBH}}(z)$, because it produces a number of low-mass black holes ($3 - 5 M_{\odot}$), which merge on a longer timescale than more massive black holes. For BHNSs, the effect of the core-collapse SN model is mixed and depends on the choice of the a_{CE} parameter.

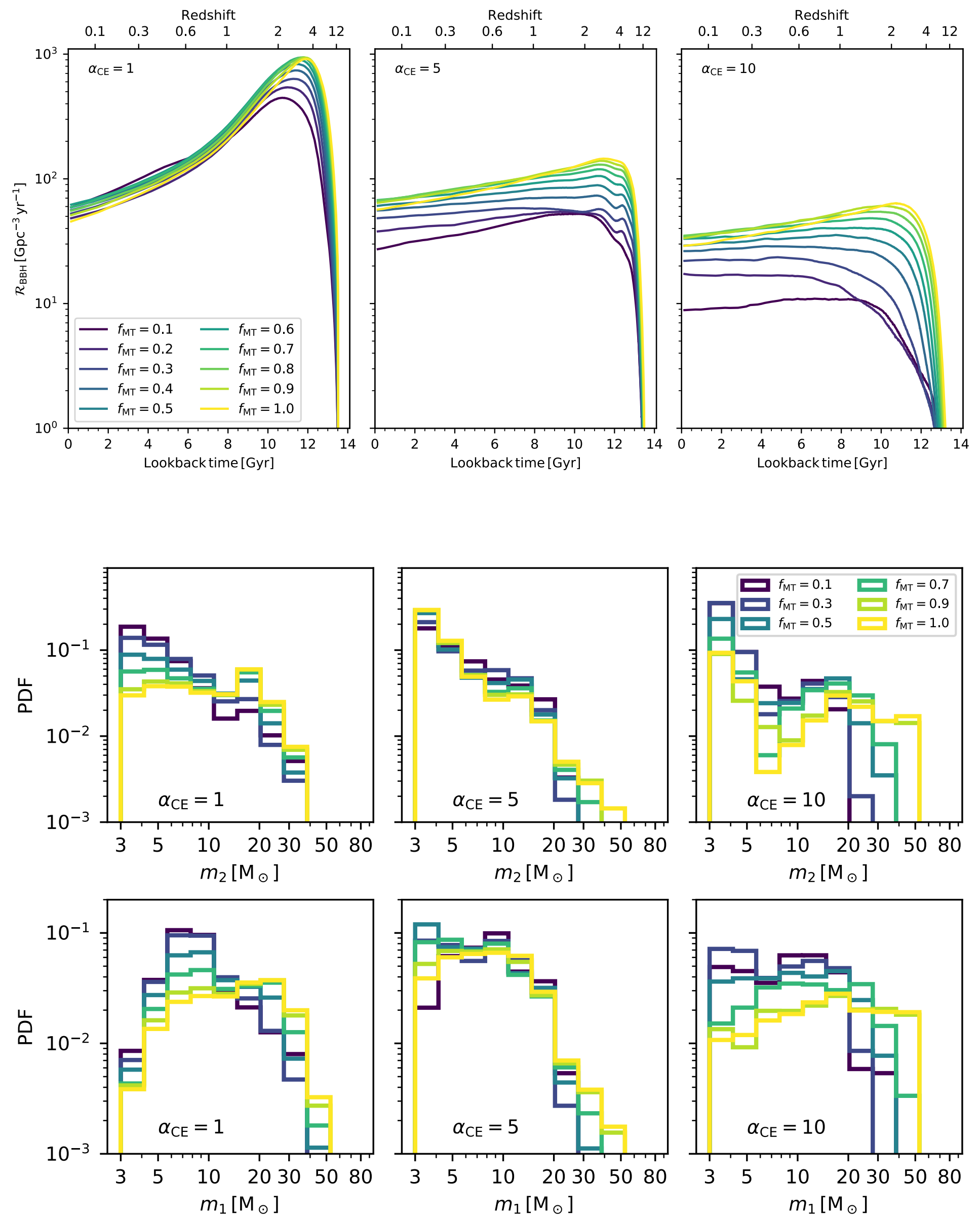


Comparison with cosmological simulations

- The merger rate density in the local Universe is a factor of $\sim 3\text{--}5$ higher in [Mapelli & Giacobbo \(2018\)](#) than in this work. This difference is due to the cosmic SFR of the **ILLUSTRIS** cosmological simulation, which is a factor of $\sim 2\text{--}2.5$ higher in the local Universe than the one given by [Madau & Fragos \(2017\)](#), and to the metallicity evolution which has a larger contribution from metal-poor stars.
- The results of cosmoRate are more similar to those reported in [Artale et al. \(2020\)](#). However, the cosmic SFR of the **EAGLE** is significantly lower than the one measured by [Madau & Fragos \(2017\)](#). This is compensated by the fact that the eagle average metallicity in the local Universe is lower.

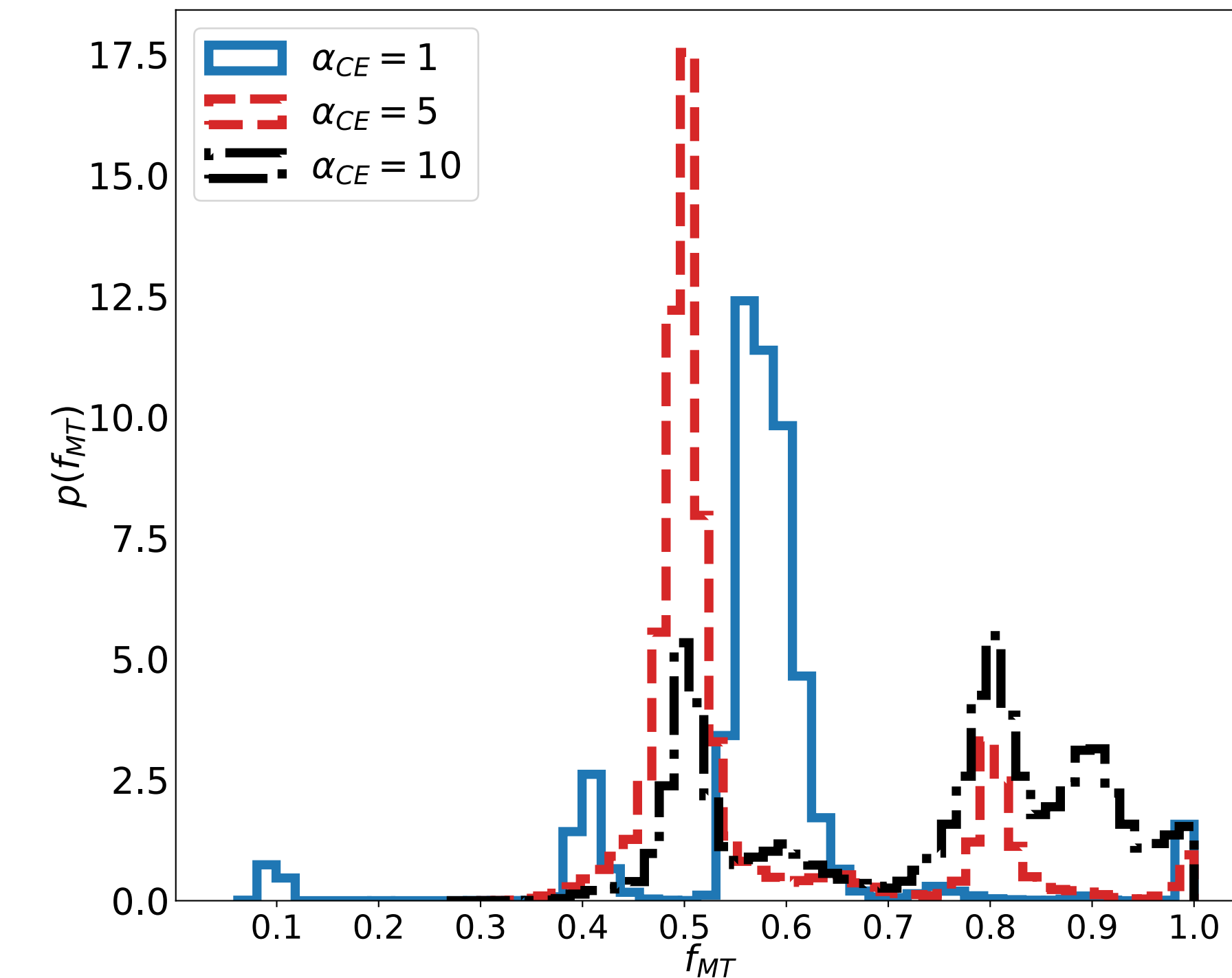


Parameter posteriors



Bouffanais et al. 2020

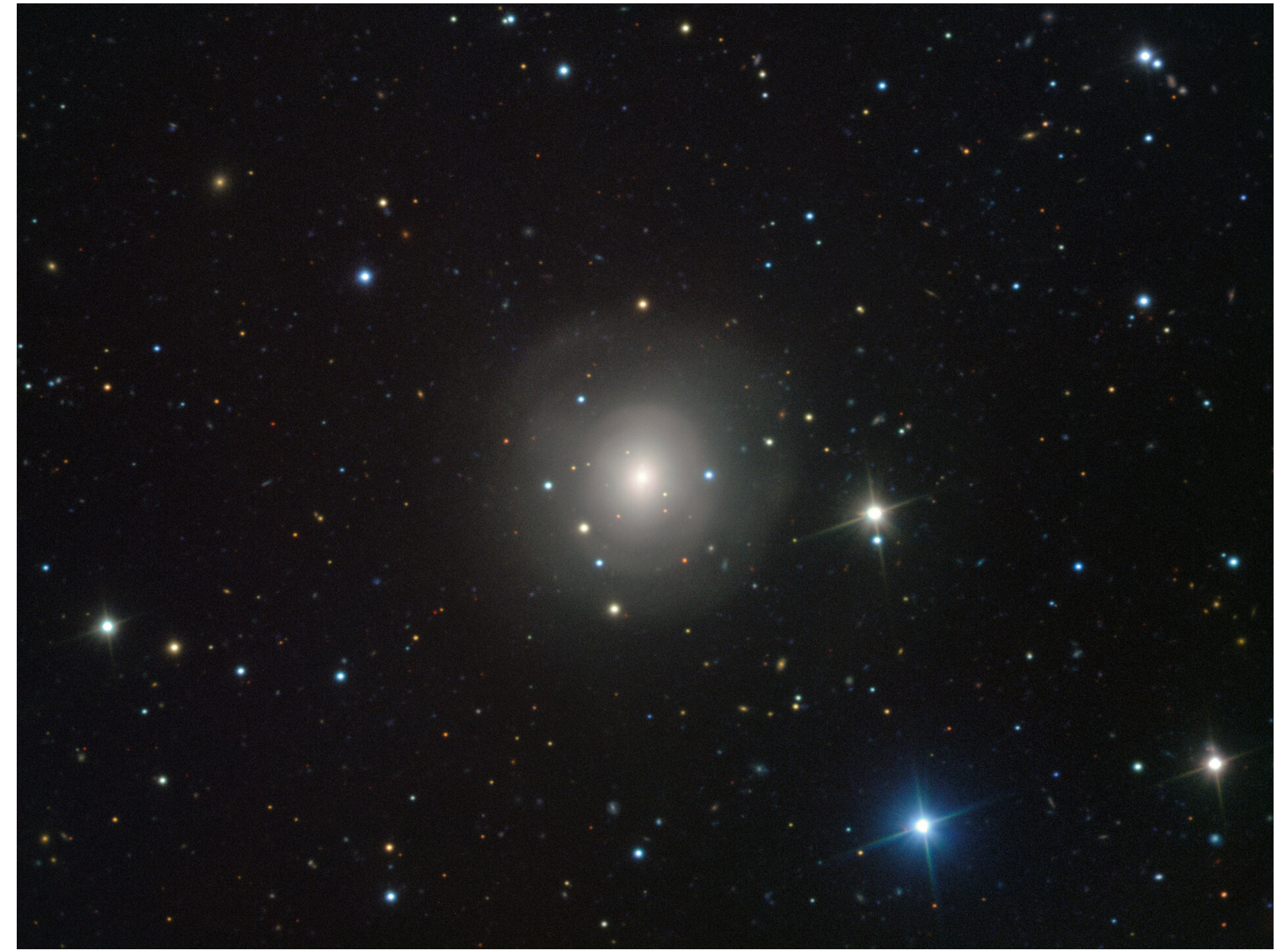
Bayesian
hierarchical
model



almost zero support for values of $f_{\text{MT}} \leq 0.3$. This result holds for all the values of α_{CE}

Future developments: Host galaxies of compact binary mergers

- I will focus on the properties of host galaxies of compact binary mergers
- It has been vastly done before with cosmological simulation (e.g. [Artale et al. 2019](#))
- However, we want to do that by means of a semi-analytic model



NGC 4993: [https://www.esa.int/ESA_Multimedia/Images/2017/10/
New_source_in_galaxy_NGC_4993](https://www.esa.int/ESA_Multimedia/Images/2017/10/New_source_in_galaxy_NGC_4993)

This red: 176 14 33